



Petrogenesis and Ni–Cu sulphide potential of mafic–ultramafic rocks in the Mesoproterozoic Fraser Zone within the Albany–Fraser Orogen, Western Australia

W.D. Maier^{a,*}, R.H. Smithies^b, C.V. Spaggiari^b, S.J. Barnes^c, C.L. Kirkland^{b,1}, S. Yang^d, Y. Lahaye^e, O. Kiddie^f, C. MacRae^g

^a School of Earth and Ocean Sciences, Cardiff University, CF10 3AT, UK

^b Geological Survey of Western Australia, Perth, Australia

^c CSIRO Mineral Resources, Kensington, WA, Australia

^d Oulu Mining School, University of Oulu, Finland

^e Geological Survey of Finland, Espoo, Finland

^f Creasy Group, 8 Kings Road, West Perth 6005, W.A., Australia

^g CSIRO Mineral Resources, Clayton, Victoria, Australia

ARTICLE INFO

Article history:

Received 28 September 2015

Revised 22 March 2016

Accepted 4 May 2016

Available online 12 May 2016

Keywords:

Albany Fraser Orogen

Nova Ni–Cu deposit

Magmatic sulphides

Basalt

Australia

ABSTRACT

The Albany Fraser Orogen is located along the southern and southeastern margins of the Archean Yilgarn Craton. The orogen formed during reworking of the Yilgarn Craton, along with variable additions of juvenile mantle material, from at least 1810 Ma to 1140 Ma. The Fraser Zone is a 425 km long and 50 km wide geophysically distinct belt near the northwestern edge of the orogen, hosting abundant sills of predominantly metagabbroic non-cumulate rocks, but including larger cumulate bodies, all emplaced at c. 1300 Ma. The gabbroic rocks are interpreted to have crystallised from a basaltic magma that had ~8.8% MgO, 185 ppm Ni, 51 ppm Cu, and extremely low contents of platinum-group elements (PGE, <1 ppb). Levels of high field-strength elements (HFSE) in the least enriched rocks indicate that the magma was derived from a mantle source more depleted than a MORB source. Isotope and trace element systematics suggest that the magma was contaminated (ϵ_{Nd} 0 to –2 throughout, La/Nb around 3) with small (<10%) amounts of crust before and during ascent and emplacement. Larger bodies of cumulate rocks show evidence for additional contamination, at the emplacement level, with country-rock metasedimentary rocks or their anatectic melts. The area has been the focus of considerable exploration for Ni–Cu sulphides following the discovery of the Nova deposit in 2012 in an intrusion consisting of olivine gabbroic, noritic and peridotitic cumulates, interlayered with metasedimentary rocks belonging to the Snowys Dam Formation of the Arid Basin. Disseminated sulphides from a drillcore intersecting the structurally upper portion of the intrusion, above the main ore zone, have tenors of ~3–6.3% Ni, 1.8–6% Cu and mostly <500 ppb PGE, suggesting derivation from magma with the same composition as the regional Fraser Zone metagabbroic sills, at R factors of ~1500. However, the Nova rocks tend to have higher ϵ_{Sr} (38–52) and more variable $\delta^{34}\text{S}$ (–2 to +4) than the regional metagabbros (ϵ_{Sr} 17–32, $\delta^{34}\text{S}$ around 0), consistent with the geochemical evidence for enhanced crustal assimilation of the metasedimentary country-rock in a relatively large magma staging chamber from which pulses of sulphide bearing, crystal-charged magmas were emplaced at slightly different crustal levels. Preliminary investigations suggest that the critical factors determining whether or not Fraser Zone mafic magmas are mineralised probably relate to local geodynamic conditions that allow large magma chambers to endure long enough to sequester country-rock sulphur.

© 2016 The Authors. Published by Elsevier B.V. This is an open access article under the CC BY license (<http://creativecommons.org/licenses/by/4.0/>).

* Corresponding author.

E-mail address: MaierW@cardiff.ac.uk (W.D. Maier).

¹ At: Center for Exploration Targeting – Curtin Node, Department of Applied Geology, Western Australian School of Mines, Faculty of Science and Engineering, Bentley, Perth, Australia.

1. Introduction

The Neoproterozoic to Mesoproterozoic Albany–Fraser Orogen (AFO), located along the southern and southeastern margins of the Archean Yilgarn Craton (Fig. 1), remains one of the least

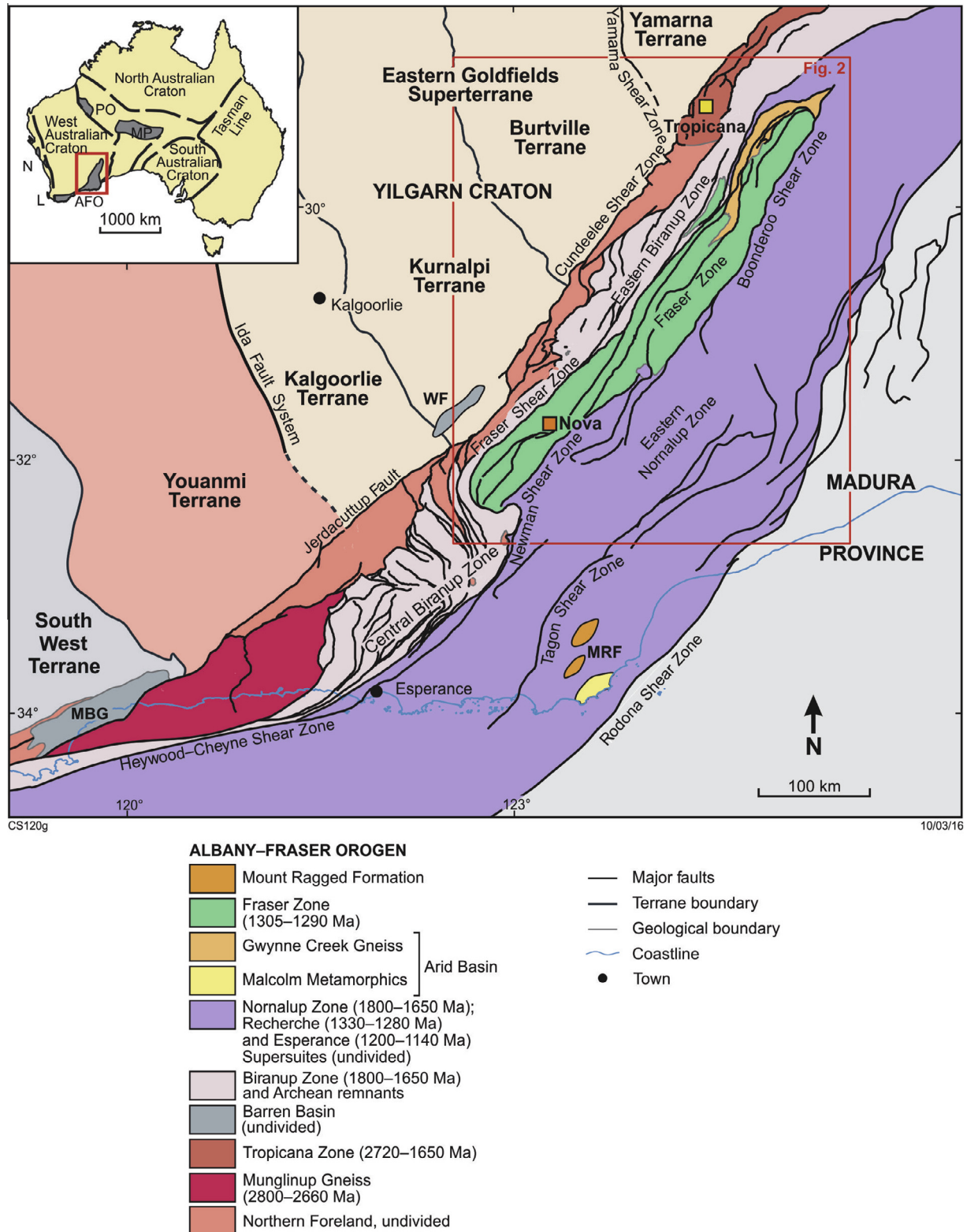


Fig. 1. Simplified, pre-Mesozoic interpreted bedrock geology of the east Albany–Fraser Orogen and tectonic subdivisions of the Yilgarn Craton. Modified from [Smithies et al. \(2013\)](#).

understood and least explored geological domains of Western Australia. The discovery of the Nova Ni–Cu sulphide deposit within the distinct, orogen-parallel and fault-bounded ‘Fraser Zone’ in 2012 ([Bennett et al., 2014](#)) has led to considerable exploration activity in the area, based on the premise that ore deposits often tend to occur in clusters. Nevertheless, because of limited outcrop

and a complex structural evolution, exploration of this extensive greenfields region for magmatic Ni–Cu sulphides remains in its infancy. In addition, emerging geological models for the region are establishing a potential for a range of other mineralisation styles (e.g. orogenic gold, VMS/VHMS, Broken Hill type etc.) yet to be tested. In this paper, we examine the composition of the

mafic–ultramafic rocks of the Fraser Zone including those within the disseminated-sulphide bearing portion above the main ore zone of the Nova deposit. We use these data to evaluate the petrogenesis of the rocks hosting the mineralisation and the magmatic sulphide ore potential of this region of the Albany–Fraser Orogen.

2. Regional setting

The Albany–Fraser Orogen is dominated by rocks formed through Neoproterozoic to Mesoproterozoic events that reworked the southern Yilgarn Craton margin (Kirkland et al., 2011a; Spaggiari et al., 2014a). Mesoproterozoic tectonism is expressed by the Albany–Fraser Orogeny, which took place in two stages: 1330–1260 Ma (Stage I) and 1225–1140 Ma (Stage II) (Clark et al., 2000; Spaggiari et al., 2015). The orogen comprises two main tectonic units – the Northern Foreland and the Kepa Kurl Booya Province – both with an evolution involving the modification of an Archean Yilgarn-like source accompanied by injection of juvenile Proterozoic material (Spaggiari et al., 2015; Kirkland et al., 2011a). The eastern boundary of the Albany–Fraser Orogen, and the limit of Yilgarn Craton reworked crust, is defined by the Rodona Shear Zone, which separates the orogen from the Madura Province (Fig. 1; Spaggiari et al., 2012, 2015; Smithies et al., 2015).

The Northern Foreland is dominated by Neoproterozoic orthogneisses of the Yilgarn Craton, deformed and metamorphosed during Mesoproterozoic tectonic events. The protoliths to these rocks formed during several magmatic events (Spaggiari et al., 2011) that are directly comparable to magmatic events elsewhere in the Yilgarn Craton (Cassidy et al., 2006; Mole et al., 2012).

The Kepa Kurl Booya Province lying immediately to the south and east of the Northern Foreland, includes the Tropicana, Biranup, Fraser and Nornalup Zones (Spaggiari et al., 2009; Occhipinti et al., 2014). The Tropicana Zone is dominated by Neoproterozoic rocks interpreted to be derived from the Yilgarn Craton, but with a different structural and metamorphic history to those of the Northern Foreland (Occhipinti et al., 2014; Tyler et al., 2014). The Biranup Zone comprises largely mid-crustal rocks, including orthogneisses and metagabbro with ages of c. 1810–1625 Ma, and isolated remnants of Yilgarn Craton rocks (Spaggiari et al., 2015; Kirkland et al., 2011a). The Nornalup Zone constitutes the southern- and eastern-most tectonic unit of the Kepa Kurl Booya Province and recent geochronological and Hf-isotopic data are consistent with the suggestion that the Biranup and Nornalup Zones formed through reworking of the same Archean Yilgarn-like crust (Kirkland et al., 2011a, 2014; Smithies et al., 2015).

The Kepa Kurl Booya province essentially formed by progressive magmatic recycling of Yilgarn crust together with episodic addition of juvenile (tholeiitic) material (Kirkland et al., 2011a). This occurred as the Yilgarn margin extended into an ocean-continent transition zone through several episodes including the 1810–1800 Ma Salmon Gums Event, the 1780–1760 Ma Ngadju Event and the 1710–1650 Ma Biranup Orogeny, accompanied by formation of the Paleoproterozoic Barren Basin (Spaggiari et al., 2015). This long period of tectonism culminated with the formation of a passive margin and marginal oceanic basin (part of the Madura Province), leading to the initial deposition of the Arid Basin between c. 1600 and 1400 Ma (Spaggiari et al., 2015). Magmatic recycling continued during and after subsequent convergence of the juvenile, oceanic crust of the Madura Province, during the Albany–Fraser Orogeny (Spaggiari et al., 2015; Smithies et al., 2015).

3. The Fraser Zone

Gravity data define the Fraser Zone as an approximately 425 km long, 50 km wide northeasterly trending unit (Fig. 2). Magnetic and

deep crustal seismic reflection data show that it is bounded by large shear zones forming a V-shape to approximately 13 km depth: the southeast-dipping Fraser Shear Zone and the northwest dipping linked Newman and Boonderoo Shear Zones (Spaggiari et al., 2014b). Only the southern portion of the Fraser Zone is exposed, whereas the northern portion is covered by thick sandy regolith and limestones of the Eucla Basin. The Fraser Zone is dominated by voluminous sheets of metagabbro (Fraser gabbro) and lesser metagranitic rocks, both of which have intruded sedimentary rocks of the Snowys Dam Formation of the Arid Basin (Spaggiari et al., 2015). These rocks have been deformed and metamorphosed to granulite facies, forming complex layering from both primary and secondary processes (the Fraser Range Metamorphics; Spaggiari et al., 2009, 2011; Clark et al., 2014). Ultramafic rocks appear to be less common than gabbroic rocks. They typically occur in the central portions of some of the gabbroic sills (e.g., at Mt Malcolm, Fig. 1), but also form an important component within larger cumulate bodies, including the host rocks to the Nova Ni–Cu sulphide deposit, discussed in more detail below. The Snowys Dam Formation is a sequence of upper amphibolite to granulite facies pelitic, semipelitic to calcic, locally iron- and locally sulphide-rich metasedimentary rocks with abundant layers and sills of Fraser gabbro. These rocks are interpreted to have been deposited in a foreland basin during the final stages of formation of the Arid Basin (maximum depositional age of 1332 ± 21 Ma), following accretion of the Loongana oceanic arc and Madura Province to the east by c. 1330 Ma, and just prior to intrusion of the Fraser Zone contemporaneous gabbroic and felsic rocks between c. 1305 and 1280 Ma (Spaggiari et al., 2015; Kirkland et al., 2011a; Clark et al., 2014).

The magmatic rocks form components of the 1330–1280 Ma Recherche Supersuite, the magmatic expression of Stage I of the Albany–Fraser Orogeny. The metagranitic rocks that intrude the metagabbros can be broadly subdivided into two groups. Local anatectic melts of Arid Basin metasedimentary rocks are typically peraluminous syenogranites referred to as the Southern Hill Suite (Smithies et al., 2014, 2015). Typically metaluminous granites form part of the Gora Hill Suite. These form relatively rare intrusions within the Fraser Zone but are more regionally distributed throughout the southeastern part of the Biranup Zone and the eastern Nornalup Zone. Geochemical and isotopic trends suggest that the metaluminous granites are derived through melting of Fraser gabbro-like mafic rocks (or of rocks resulting through melting of Fraser gabbro) and mixing with silicic crust (or melts thereof) formed during the earlier Biranup Orogeny (Kirkland et al., 2014; Smithies et al., 2014, 2015).

Peak granulite facies metamorphism of c. 850 °C at 7–9 kbar has been constrained in the Snowys Dam Formation in the Fraser Zone at c. 1290 Ma, coeval with magmatism, and only shortly after the sediments were deposited (Clark et al., 2014). The peak metamorphic pressures could constrain the depth (25–30 km) at which the gabbros of the Fraser Zone were intruded and thus the minimum depth of this portion of the Arid Basin. However, the P–T conditions were determined from metamorphic assemblages with a gneissic fabric (Oorschot, 2011), and could relate to post magmatic folding and crustal thickening (Smithies et al., 2013). Certainly, the available data indicate a relatively short time interval for sediment deposition, igneous crystallization, and near coeval granulite-facies metamorphism and suggest that regional magmatism was the thermal driver of metamorphism (Clark et al., 2014).

Present interpretations are that the Fraser Zone represents a structurally modified, middle- to deep-crustal 'hot zone', formed by the repeated intrusion of gabbroic magma from a mantle upwelling into quartzofeldspathic country rock (Spaggiari et al., 2015; Smithies et al., 2013; Clark et al., 2014).

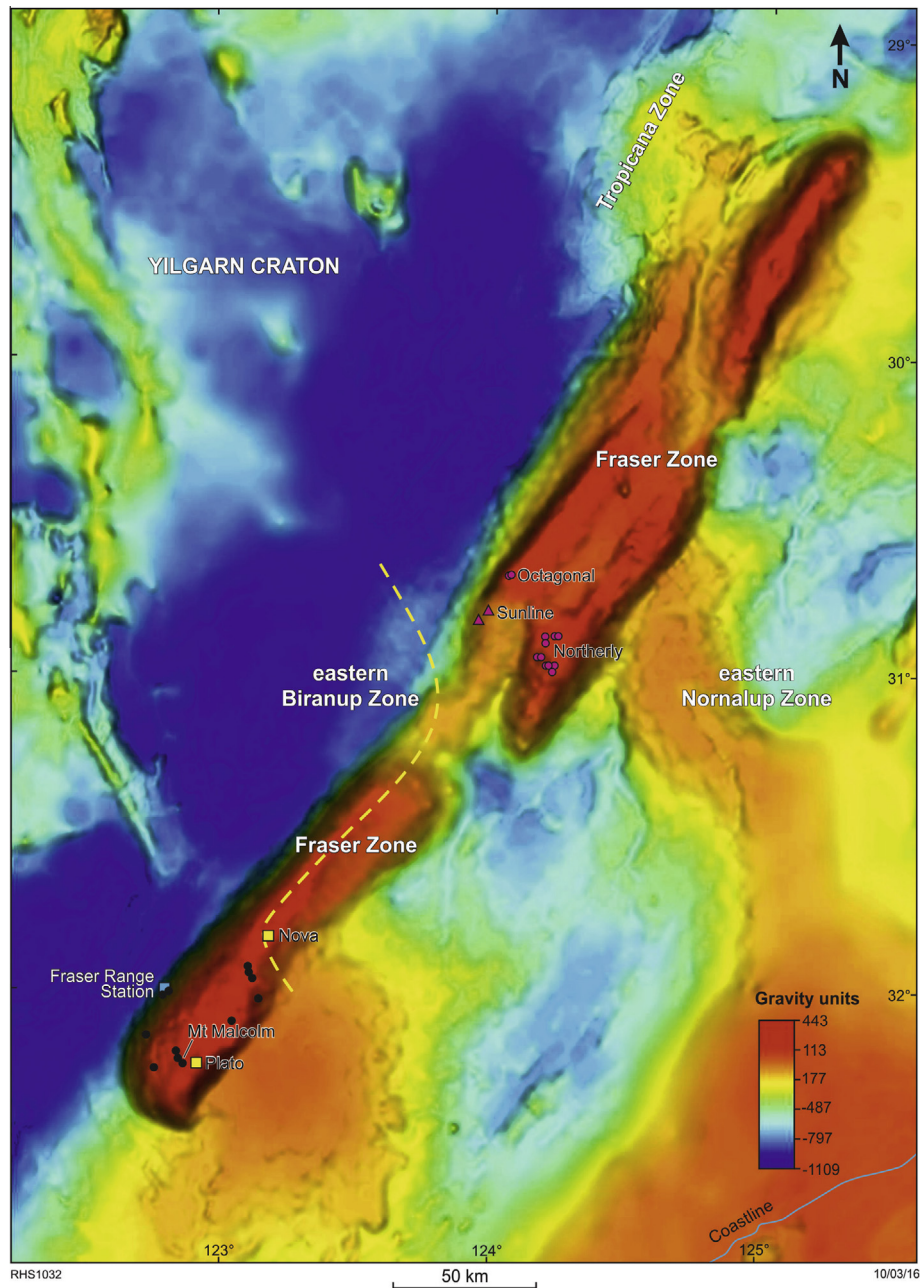


Fig. 2. Gravity image showing the full extent of the Fraser Zone, approximate limit of outcrop (west of yellow dashed line), and sample localities. Black dots are the locations of the outcrop samples reported in [Smithies et al. \(2013\)](#). Octagonal, Northerly and Sunline are Creasy Group prospects from which samples were analysed. (For interpretation of the references to color in this figure legend, the reader is referred to the web version of this article.)

4. The Nova deposit

Targeting of the Nova Ni–Cu deposit in 2012 was initially based on a geochemical soil anomaly identified from regional datasets produced by the Geological Survey of Western Australia and a magnetic feature termed ‘the Eye’. Early drilling included the first diamond hole (SFRD-0017), co-funded by the Western Australia government’s Exploration Incentive Scheme (EIS), drilled 280 m into mafic–ultramafic rocks carrying disseminated Ni–Cu sulphides ([Gollam, 2012](#); [Bennett et al., 2014](#)). Based on similarities in sulphide composition, this material is interpreted by us to represent the upper portion of the intrusion that contains the Nova massive and net-textured sulphide mineralisation

interlayered with mafic–ultramafic rocks towards its base. The intrusion has since been extensively drilled and appears to comprise a sequence of gabbroic and ultramafic rocks of >400 m thickness and at least 900 m width, interlayered with pelitic metasedimentary rocks of the Snowys Dam Formation ([Fig. 3](#)). These rocks have undergone significant deformation and granulite-facies metamorphism. In February 2013, Sirius Resources announced the Bollinger discovery, a dominantly flat lying body located to the east of the Nova deposit and connected to the Nova deposit by an interpreted feeder zone. The combined resource stands at 14.6 Mt of ore at 2.2% Ni, 0.9% Cu, and 0.08% Co, with a contained 325,000 t of nickel, 134,000 t of copper; and 11,000 t of cobalt ([Bennett et al., 2014](#)).

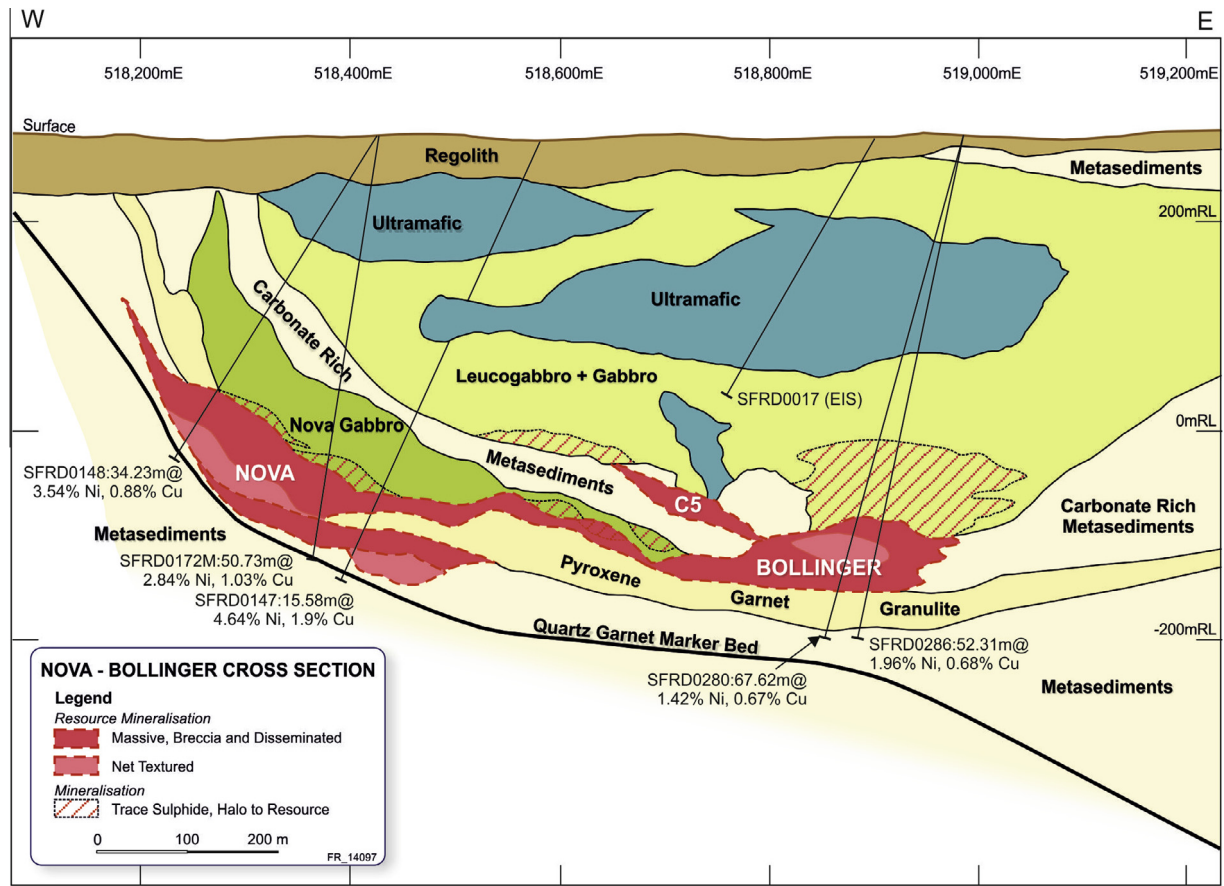


Fig. 3. Simplified geological cross section of Nova deposit. Redrawn after profile provided in written com. by P. Parker, 12 Dec. 2015.

5. Sample material and analytical methods

In total we have analysed more than 100 mafic–ultramafic samples from the Fraser Zone, amongst them 26 samples from the SFRD-0017 drill core located just above the main ore zone at the Nova deposit (see [Electronic Appendix 1](#)). The Nova samples are largely unaltered aside from partial serpentinisation of olivine. To help better constrain petrogenetic processes throughout the Fraser Zone, and lead to more effective Ni–Cu exploration models in that region, the Creasy Group of Companies has provided unaltered rock chips of a sample suite comprising a representative range of mafic and ultramafic rocks from exploration tenements within portions of the Fraser Zone approximately 130–150 km to the north-east of Nova that are under cover, as well as access to diamond core of sulphide bearing metasedimentary rocks of the Snowys Dam Formation, from their Sunline Prospect within these tenements (Fig. 2).

For the purpose of identifying the geochemical signatures of any possible contaminant within the rocks, we complimented our dataset with 70 analyses of granitic and metasedimentary rocks from elsewhere within the Fraser Zone and more regionally within the east Albany–Fraser Orogen, considered to be representatives of all known major crustal lithologies. All analyses can be obtained from the Geological Survey of Western Australia WACHEM database (<http://geochem.dmp.wa.gov.au/geochem/>), along with analytical details. Samples were prepared for analysis at GSWA using a jaw crusher followed by milling in a tungsten carbide mill. The mill was tested for possible contaminants, with only W and Co being significant. Major elements were determined at ALS Laboratories (Perth) by wavelength-dispersive X-ray fluorescence (XRF)

on fused disks. Trace element concentrations were determined at Geoscience Australia by inductively coupled plasma-mass spectrometry (ICP-MS). Precision and accuracy has been monitored by in-house reference materials KG1 and BB1. Precision has been estimated by calculating the percent relative standard deviation (or covariance) for each RM. Precision for major elements is better than 1% of the reported values, and precision for trace elements is better than 10% of the reported values. Accuracy has been assessed by comparing the recommended analyte value (Morris (2007) – GSWA record 20017/14 – with the average analyte concentration using the formula: $100 * \text{ABS}((\text{average-recc})/(\text{average} + \text{recc}))$. HRD values are mostly <10.

Platinum-group element concentrations were determined by Ni-sulphide fire assay followed by Te co-precipitation and ICP-MS at the University of Quebec at Chicoutimi, Canada. Analytical details are given in [Barnes et al. \(2010\)](#). All data as well as estimates of precision and accuracy are provided in [Electronic Appendix 2](#).

In situ S isotope analyses of pyrrhotite were performed using a Nu Plasma HR multicollector ICPMS at the Geological Survey of Finland in Espoo together with a Photon Machine Analyte G2 laser microprobe. Samples were ablated in He gas (gas flows = 0.4 and 0.1 l/min) within a HelEx ablation cell ([Müller et al., 2009](#)). S isotopes were analyzed at medium resolution. During the ablation the data were collected in static mode (^{32}S , ^{34}S). Single spots of pyrrhotite were ablated at a spatial resolution of 40 micrometers, using a fluence of 0.83 J/cm² and a repetition rate of 5 Hz. The total S signal obtained for pyrrhotite was typically below 2 V. Under these conditions, after a 20 s baseline, 30–50 s of ablation is needed to obtain an internal precision of $^{34}\text{S}/^{32}\text{S} \leq \pm 0.00001$ (2σ). One in-house pyrrhotite standard (Polopo) has been used for external

standard bracketing. Two pyrite standards have been used for quality control (PPP-1, Gilbert et al., 2014, and in house standard Py1). An average $\delta^{34}\text{S}_{\text{CDT}} (\text{‰})$ value of $-0.85 \pm 0.22\text{‰}$ (2σ , $n = 5$) for Py1 was obtained, which is consistent with the value measured by gas mass spectrometry of $-0.6 \pm 1.2\text{‰}$ (2σ). For PPP-1, we obtained an average value of $4.6 \pm 0.4\text{‰}$ (2σ , $n = 12$), slightly lower than the reported value of $5.3 \pm 0.2\text{‰}$ (2σ) by Gilbert et al. (2014). Part of the difference in accuracy is related to the standard homogeneity and matrix effect between Po and Py. Results of our analyses are provided in Electronic Appendix 3.

Whole rock sulphur isotopes in sedimentary rocks were determined by Rafter GNS Sciences at the New Zealand National Isotope Centre. The samples were measured in duplicate in tin capsules with equal amounts of V_2O_5 on a EuroVector Elemental Analyzer connected to a GVI IsoPrime mass spectrometer. All results are averages and standard deviations of duplicates are reported with respect to VCDT, normalized to internal standards: R18742, R2268, and R2298 with accepted $\delta^{34}\text{S}$ values of -32‰ , $+3.3\text{‰}$, and $+8.6\text{‰}$, respectively. The external precision for this instrument is better than 0.3 for $\delta^{34}\text{S}$.

The analysis of *in situ* Sr isotopic compositions of plagioclase was conducted on a Photo Machine Analyte G2 laser microprobe coupled to a Nu Plasma HR multicollector inductively coupled mass spectrometer at the Geological Survey of Finland in Espoo. The analytical conditions are largely similar to those reported by Yang et al. (2013), who used a slightly modified methodology from that described by Ramos et al. (2004, 2005). The repeated analysis of an in-house plagioclase standard after approximate every ten measurements yielded an average $^{87}\text{Sr}/^{86}\text{Sr}$ ratio of 0.70312 ± 0.00010 (2σ , $n = 33$), which is consistent with the reference ratio of 0.70310 ± 0.00010 (2σ) determined by thermal ionisation mass spectrometry (sample Mir a, Rankenburg et al., 2004). The average value of several analyses ($n = 5$ –9) is considered to represent the bulk composition, with a standard deviation of $\leq \pm 0.00040$ (2σ). The measured isotopic ratios were then age-corrected to 1300 Ma (Reference). The data are listed in Electronic Appendix 4.

Sm–Nd isotope measurements were determined on whole-rock sample powders by isotope dilution at the University of Rennes (France) and the University of Queensland (Australia) over the course of several years. Analytical details are given in Kirkland et al. (2014), and the data including analytical errors are provided in Electronic Appendix 1.

Different phases within the samples were quantitatively analysed for Si, Mg, Ni, Fe, K, Al, Na, Co, Mn, Ti, Cr, and Ca using a JEOL 8900R electron microprobe in the CSIRO labs at Clayton, Victoria. All elements were analysed using the $K\alpha$ line except for Co which used the $K\beta$ to avoid the overlap with Fe; $K\alpha$. Standards used were San Carlos olivine [$(\text{Mg}, \text{Fe})_2\text{SiO}_4$], heazlewoodite [Ni_3S_2], hematite [Fe_2O_3], adularia [KAlSi_3O_8], magalox-spinel [MgAl_2O_4], albite [$\text{NaAlSi}_3\text{O}_8$], Co metal, rhodonite [MnSiO_3], rutile [TiO_2], chromite [Cr_2O_3], wollastonite (CaSiO_3). Oxygen was calculated by stoichiometry, based on valence. Operating conditions for the microprobe were; an accelerating voltage of 20 kV and a beam current of 15 nA. To average the composition of grains, the electron beam was defocused a same amount ($5 \mu\text{m}$) for the analyses. All analysis positions were verified as being homogeneous by viewing the backscattered electron image of the area to be analysed. All elemental analyses were corrected for atomic number (Z), absorption (A) and fluorescence (F) using a Phi-Rho-Z matrix correction procedure implemented on the JEOL 8500F. The JEOL 8500F was equipped with five wavelength dispersive spectrometers and two energy dispersive spectrometers. The compositional data and calculated detection limits based on counting statistics are listed in Electronic Appendix 5.

6. Results

6.1. Lithologies and petrography of outcrop samples

Metagabbros of the Fraser Zone form sheets of variable thickness (centimeters to hundreds of meters) within the metasedimentary host sequence. These sheets appear to thicken to the southeast where metagabbroic rocks become much more abundant than metasedimentary rocks. Outcrops show evidence (e.g., inclusions, stringers, schlieren, mingling textures) for the incorporation of metasedimentary country rock, local melts of country rock, or of contemporaneous granodiorite intrusions (Fig. 4). Thus, the metagabbros are broadly divided into hybrid rocks (further subdivided into 2 groups below) and rocks that show no field or geochemical evidence for contamination – referred to as the ‘main gabbros’. Whereas many samples of gabbro studied here show a high-grade metamorphic textural overprint and fabric, textures of the main gabbros (Fig. 5a) range from near pristine igneous intergranular to sub-ophitic and granoblastic. The full range of textures can be observed at single localities. Zones of relatively high strain may show pronounced foliation, but in many cases this is overprinted by a granoblastic texture. The main gabbros comprise fine- to medium-grained, mesocratic olivine gabbro and olivine gabbro-norite, containing 35–60% plagioclase (An55–70, semi-quantitative SEM analysis of 1 sample), up to 15% anhedral to subhedral olivine that is partially enclosed within orthopyroxene, up to 50% intergranular, poikilitic or granoblastic pyroxene, with clinopyroxene being more abundant than orthopyroxene, up to 5% magnetite, as well as up to 10% brown biotite. In granoblastic rocks, biotite is either absent or forms flakes which may be strongly aligned with the gneissic foliation. Brown hornblende is a notable component of most of the rocks, forming up to 20% of the mode. It rims biotite and pyroxene, commonly as granoblastic aggregates. Sulphides are rare and mainly confined to the Mount Malcolm locality (see Electronic Appendix 1 for GPS coordinates of this location) where they form blebs consisting of pyrrhotite, flame- and granular pentlandite, and chalcopyrite in broadly magmatic proportions.

The hybrid gabbros can be sub-divided into ‘Group 1’ and ‘Group 2’, based largely on geochemistry (Smithies et al., 2013). Both groups are fine- to medium-grained, mesocratic rocks, commonly showing well developed granoblastic textures. In some cases they preserve an igneous intergranular to sub-ophitic texture. In contrast to the main gabbros, they typically contain little or no olivine and some samples contain rare interstitial quartz. In some samples from the Wyrallinu Hill locality garnet poikiloblasts up to 6 mm in size have been observed. Although hornblende is typically brown, it can range to brown-green to green. Some Group 2 hybrid gabbros are texturally very heterogeneous, comprising fine-grained granoblastic domains enclosing felsic domains forming layers, elongate blebs or wisps up to 3 cm long and consisting of plagioclase (commonly antiperthitic), lesser amounts of quartz and rare perthite (Fig. 4).

6.2. Lithologies and petrography of the Nova drill core SRF0017

The Nova samples comprise lherzolite, wehrlite, websterite, gabbro-norite and anorthosite. The rocks are mostly medium grained (Fig. 5b–h), but some of the gabbro-noritic and noritic rocks are fine-grained. Contacts between the medium grained and fine grained lithologies tend to be gradational on the scale of mm to cm. In the lower portion of the drill core the metagabbro is interlayered with metasedimentary rocks (Fig. 6h), and in addition there are several decimetre-scale dolerite veins. Most rocks are relatively unaltered, or are moderately altered in the form of

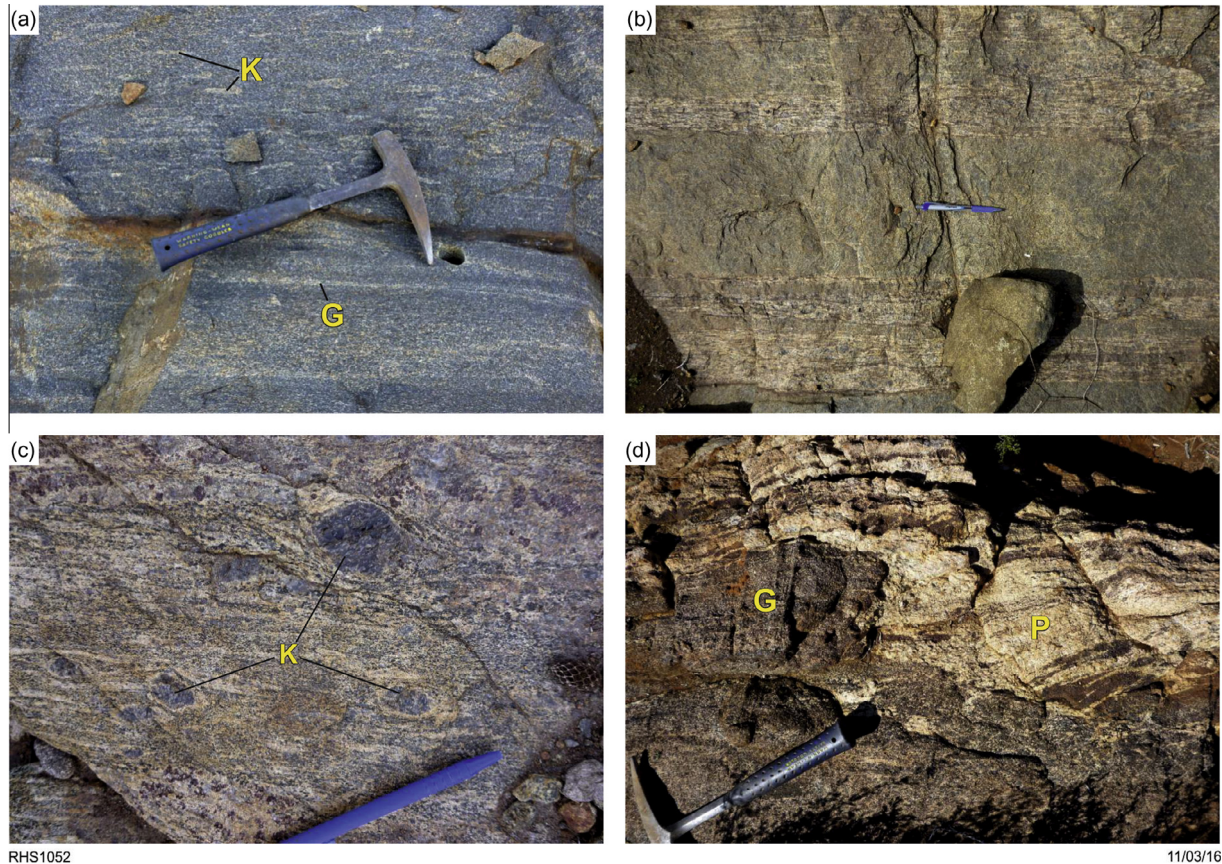


Fig. 4. Field photos of the Fraser Range Metamorphics, southern Fraser Zone. (a) Metagabbro with wispy and thin layers of granitic material (G), and sparse K-feldspar phenocrysts (K); Phil's Quarry, (b) Metagabbro (dark) interlayered with granite (pale); gully exposure at Wyranilu Hill, (c) K-feldspar porphyroclasts (K) in hybrid metagabbroic to metagranitic rocks; Wyranilu Hill, (d) Gabbro (G) intruded into psammitic gneiss (P) of the Snowys Dam Formation, near Yardilla prospect.

sericitisation of plagioclase, locally abundant brown hornblende, and serpentine veins in olivine. The textures are typically granular, with grain boundary angles of $\sim 120^\circ$, but harzburgites consisting of orthopyroxene oikocrysts and olivine chadacrysts also occur (Fig. 5c). Gabbro-noritic sample GSWA 201255 contains fine grained domains of granular norite embedded in a matrix of medium- to coarse grained gabbro-norite (Fig. 5). Ultramafic cumulates show a range of lithologies, the most common being poikilitic lherzolite with clinopyroxene and subordinate orthopyroxene oikocrysts up to 1 cm in diameter. These are interlayered with granular lherzolite containing sub-equant olivine and orthopyroxene typically 1–2 mm in diameter, and orthopyroxenite and websterite with minor olivine and patches of interstitial plagioclase. Clinopyroxene is typically rimmed with brown hornblende. The interstitial space in the pyroxene-rich lithologies is typically occupied by a distinctive symplectic intergrowth of pyroxene (probably inverted pigeonite) and plagioclase. Orthopyroxene and clinopyroxene typically constitute 10–20% of the rock, except in websterite. A metamorphic overprint is apparent in the form of sub-grain coronas of pyroxene around olivine, abundant small grains of green and brown spinel, and symplectic intergrowths of pyroxene and plagioclase with secondary green spinel (Fig. 5b). These textures resemble those found in ultramafic rocks of the Niquelandia intrusion, Brazil (Fornoni Candia et al., 1989) and the Giles intrusions in central Australia (Glikson et al., 1996; Maier et al., 2015) where they were interpreted to reflect Al-transfer from plagioclase to spinel during high pressure cooling. Plagioclase is mostly intercumulus, but subhedral cumulus grains also occur. Brown mica and apatite are accessory phases and chromite is a ubiquitous trace phase in the olivine cumulates. Sulphides constitute up to approximately 10% of the

rock, either in the form of intercumulus or drop-like grains, mostly smaller than 0.5 mm. In some of the rocks there appear to be 2 distinct modes of sulphide occurrence. For example, the bulk of sample GSWA 201255 shows low amounts of interstitial and vein-style sulphides with a high proportion of chalcopyrite in coarse grained gabbro-norite, whereas fine- to medium grained granular textured noritic and pyroxenitic domains that appear to be autoliths are more strongly mineralised containing a typically magmatic assemblage of pyrrhotite, granular pentlandite and chalcopyrite (Figs. 5f, g and 7).

6.3. Mineral compositions of the Nova deposit

The compositions of olivine, orthopyroxene, clinopyroxene, plagioclase and spinel were determined in 10 samples of drill core SRFR0017 intersecting the upper portion of the Nova intrusion, including norite, gabbro-norite, and harzburgite. The forsterite content of olivine varies from ~ 80 to 83, with Ni contents from ~ 900 to 1700 ppm (average 1130 ppm, Fig. 8). The harzburgites have slightly higher Fo than the norites and gabbro-norites, but Ni contents of olivine broadly overlap with the gabbroic rocks. Within individual rock types there is little systematic compositional variation with height (Fig. 9). In general, most Nova olivines are relatively depleted in Ni compared to olivines from layered intrusions and basic-ultrabasic lavas globally (Fig. 8).

Orthopyroxene has Mg# 71–84 and up to 0.62% Cr_2O_3 in harzburgite, but $<0.1\%$ Cr_2O_3 in norite and olivine gabbro. Al_2O_3 contents vary from 1.5% in norite to 4% in gabbro-norite and harzburgite. Clinopyroxene has Mg# 79–89, with up to 1.27%

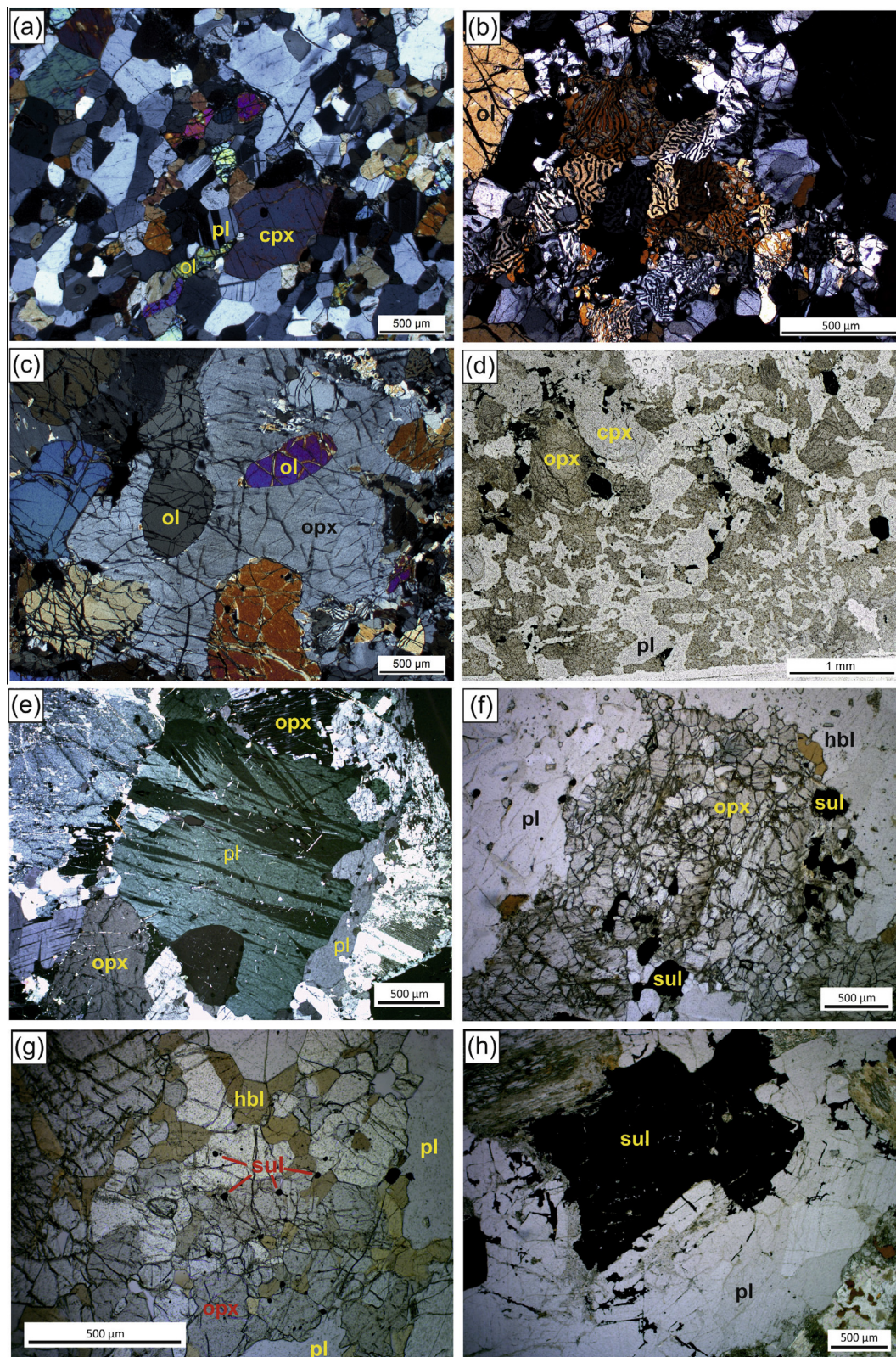


Fig. 5. Photomicrographs of Fraser Zone rocks. (a) Mt. Malcolm gabbronorite, sample GSWA 183654. (b) Lherzolite from Nova, sample GSWA 201236 (96 m). Note symplectitic intergrowth of pyroxene and plagioclase with secondary green spinel. (c) Harzburgite from Nova, core SRFR0017, sample GSWA 201236, 96 m. (d–h) Gabbronorite from Nova, core SRFR0017, sample GSWA 201255, 56.85 m. Note heterogeneous texture in (d), with domains of relatively fine grained norite interpreted as fragments, deformation of plagioclase expressed by bent and spindle-like twin lamellae in (e), fragments of fine grained sulphide rich orthopyroxenite in (f and g), and remobilised vein-style sulphides in the periphery of intercumulus sulphide (h).

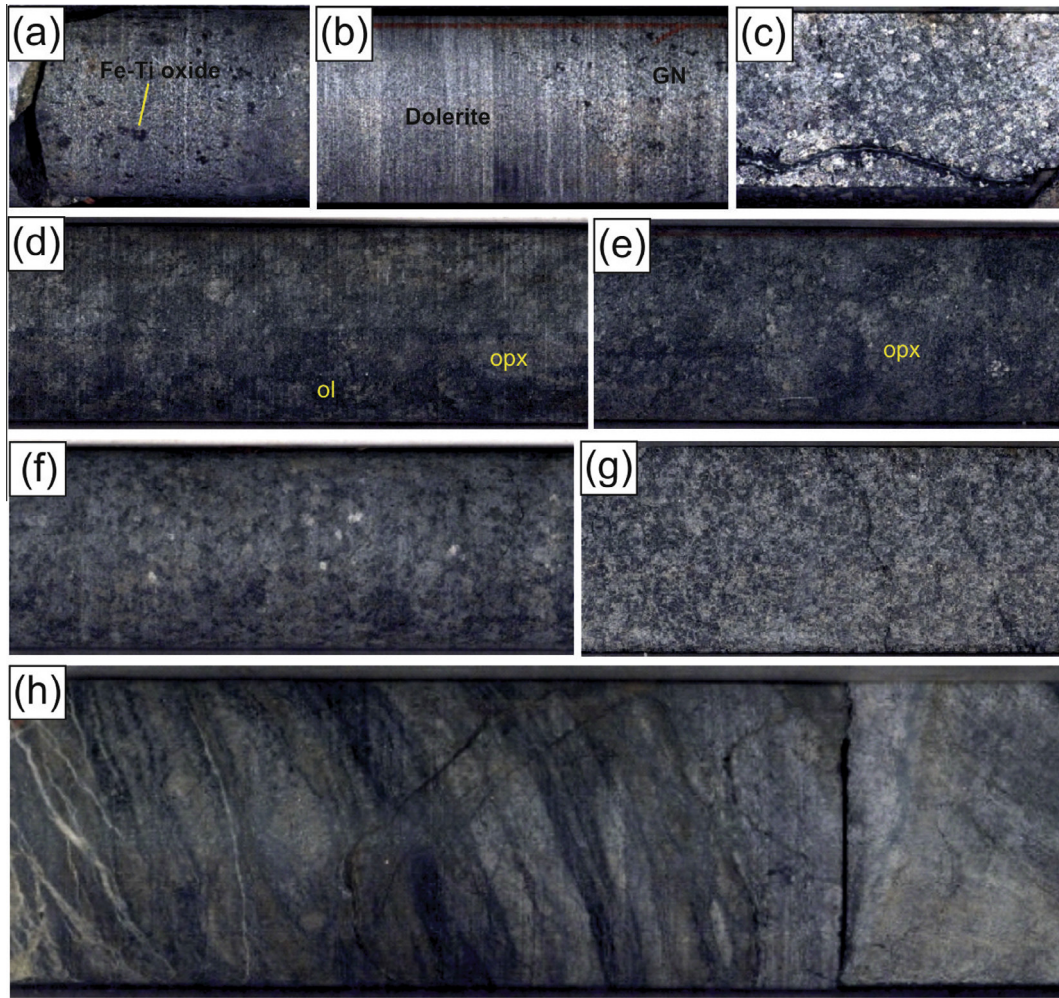


Fig. 6. Lithologies in drill core SRFR0017 at Nova. (a) Gabbronorite, 71–71.2 m. (b) Contact between dolerite and medium grained gabbronorite, 91.2 m. (c) Peridotite, 100.8 m. (d) Poikilitic peridotite, 188–194 m. (e) Poikilitic peridotite, 200.9 m. (f) Peridotite, 218.4 m. (g) Peridotite, 278.7 m. (h) Banded metasedimentary rock (chlorite-garnet schist), 220 m. Width of drill core in all images is 4.7 cm.

Cr_2O_3 in harzburgite. Cumulus plagioclase has An 62–78, except for one sample of gabbronorite that has An 86–89.

6.4. Lithophile geochemistry

Average compositions of the main gabbro and the Group 1 and 2 hybrids, as well as peridotites and gabbronorites from Nova and the Creasy Group of companies are given in Table 1. Major and trace element variations in the mafic ultramafic rocks are plotted against MgO in Fig. 10. The compositions of some key minerals are also plotted, based on microprobe data from Nova samples (Electronic Appendix 5).

The main gabbros from the Fraser Zone have on average 8.8% MgO, 185 ppm Ni and 240 ppm Cr, consistent with basaltic compositions. The hybrid gabbros plot towards low MgO, Al_2O_3 and CaO, and high SiO_2 .

The Nova cumulates have up to 35% MgO and their compositions are mainly controlled by modal variations in plagioclase, olivine, clinopyroxene and orthopyroxene, as reflected by the well defined negative correlations in the $\text{Al}_2\text{O}_3/\text{MgO}$, CaO/MgO and Sr/MgO plots (Fig. 10). The Cr/MgO and Ni/MgO plots show considerably more scatter, likely due to the presence of chromite and sulphide. The ultramafic samples from the Creasy Group of companies are more MgO rich than the most magnesian Nova samples, and they are richer in Cr and Ni. However, many of the

gabbroic samples from the Creasy Group sample suite have compositions similar to those of the main gabbros of the Fraser Zone

Incompatible elements are plotted in Fig. 10g and h. The main gabbros have average contents of 106 ppm Zr, 1.2% TiO_2 , and 0.6% K_2O (the latter not shown) with the hybrid gabbros being notably enriched in these elements, at up to 800 ppm Zr, 2% TiO_2 , and 3.5% K_2O . The mafic and ultramafic rocks from Nova and the Creasy Group of companies have much lower concentrations of these trace elements, i.e., 5–20 ppm Zr, and <0.5% K_2O and TiO_2 .

The bulk of the main gabbros show limited variation in terms of such differentiation indexes as Cr/V (1–3), and Mg# (0.55–0.65). The hybrid gabbros extend to lower Cr/V and Mg#, whereas the Nova cumulates form a distinct group with higher Mg# and Cr/V. The highest Cr/V and Mg# occur in the Nova and Creasy Group peridotites which show some overlap, although the Creasy Group samples have higher average Cr/V.

Compared to MORB, the main gabbros are strongly enriched in LILE and LREE, but most have MORB-like concentrations of Nb (and Ta), Zr, Hf and HREE (Fig. 11). On a N-MORB-normalized trace element variation diagram, the two samples with anomalously low incompatible trace element concentrations (GSWA 183624, 183654 – red lines in Fig. 11) show similar, but less enriched trace element patterns to those of the other rocks. The peridotites and gabbronorites from Nova show remarkably similar patterns to the Fraser Zone main gabbros, but the patterns of the Nova rocks

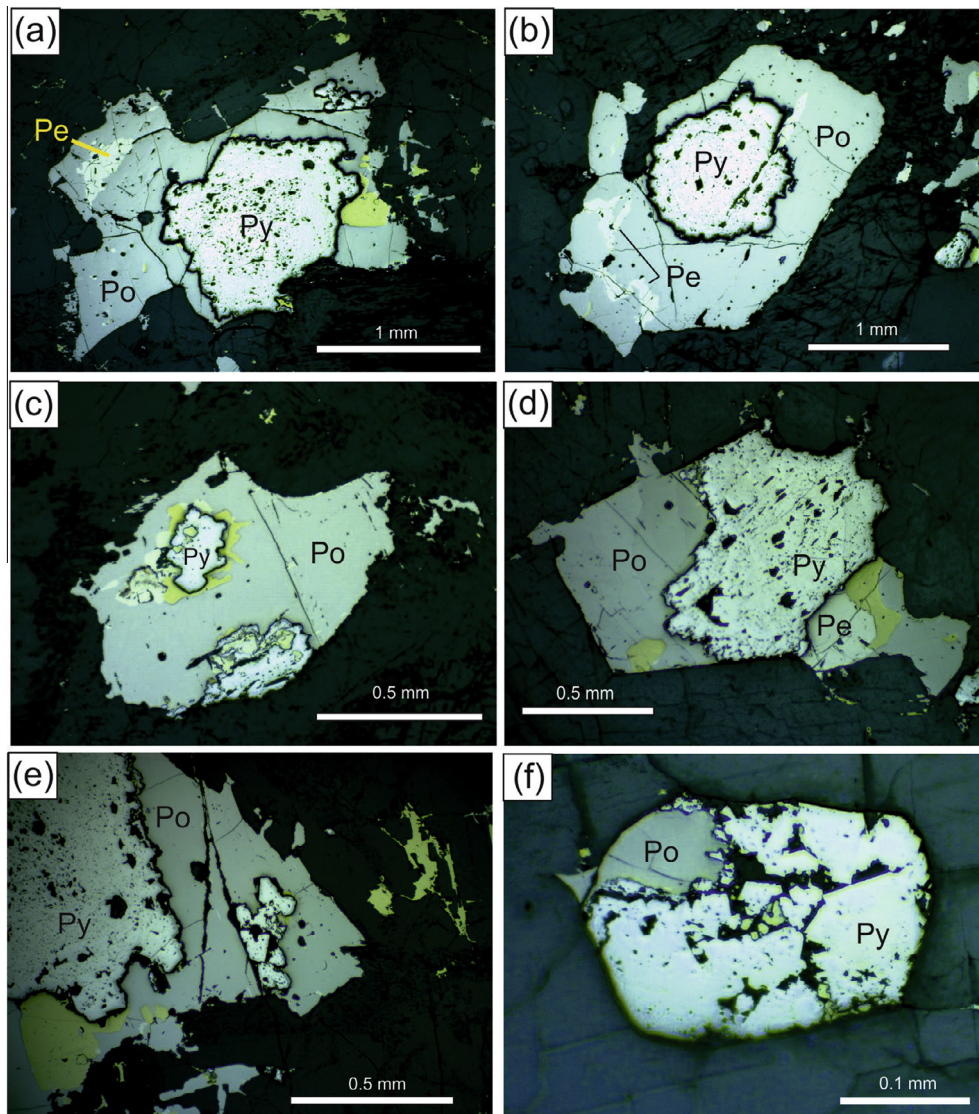


Fig. 7. (a–f) Sulfides in Nova drill core SFRD0017, sample GSWA 201255, 56.85 m. Note replacement of pyrrhotite, pentlandite and chalcopyrite by gangue and pyrite.

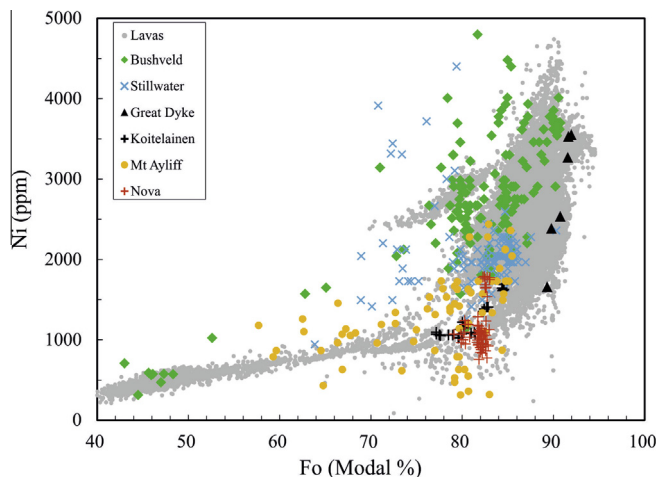


Fig. 8. Plot of Ni vs Fo in Nova olivine, compared to layered intrusions globally (data compiled from Teigler and Eales, 1996; Maier and Eales, 1997; Lightfoot and Naldrett, 1983; Raedeke, 1982; E Hanski, unpublished data). Grey shading is data on global basic-ultrabasic lavas, from Sobolev et al. (2011).

are somewhat more fractionated, with more pronounced negative Nb anomalies, positive Sr and negative Zr anomalies, as well as lower bulk trace element contents.

A detailed compositional profile through the upper portion of the Nova deposit, as exposed in drill core SFRD0017 is shown in Fig. 12. The profile is characterised by alternation of gabbro and peridotite, reflected in variation in MgO contents. In much of the profile the 2 rock types define distinct populations, with the ultramafic rocks containing 30–35% MgO and the gabbros 9–16% MgO. Only in the upper portion of the section, between units 5–6 and 7–8 is there some evidence for compositions intermediate between these end-members, with MgO in the gabbros reaching 20% and in the peridotite falling to 27%.

Mg# and Cr/V tend to be slightly lower in the gabbros than in the peridotites, but there is considerable overlap. The gabbros have lower Ce/Sm (3–5) than the ultramafic rocks (Ce/Sm mostly around 6), but La/Nb ratios of the 2 rock types overlap.

6.5. Chalcophile element geochemistry

Copper contents in the main gabbros and hybrid gabbros of the Fraser Zone are mostly 30–70 ppm, with an average of 51 ppm

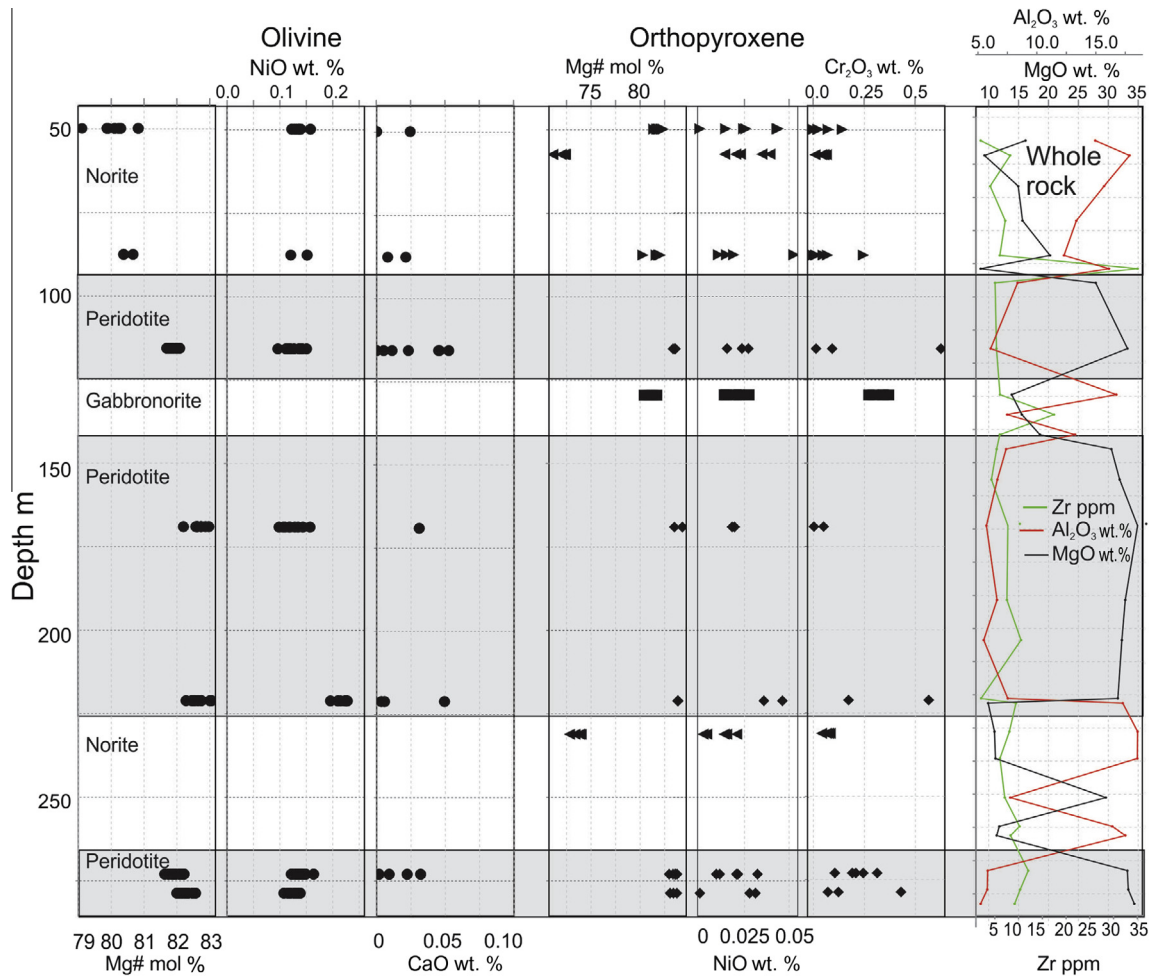


Fig. 9. Composition of orthopyroxene and olivine plotted vs height in Nova drill core SFRD0017.

(Fig. 13), significantly lower than typical N-MORB (average 73 ppm, Gale et al., 2013). Group 2 hybrid gabbros have relatively low Cu/Zr (Fig. 13c), resulting from both slightly higher Zr and lower Cu. Sulphur contents of the main gabbros and Group 1 hybrids cluster around 1000 ppm, in the range of many other MORB magmas (Wallace and Carmichael, 1992). Group 2 hybrid gabbros have systematically lower S than the main gabbros (Fig. 13b).

The Nova samples have up to 5000 ppm Cu and 4000 ppm S (Fig. 13a,b). The average Cu and S contents are significantly higher than in the Fraser Zone main and hybrid gabbros, and there is very little overlap between these populations. Notably, the gabbro-norites tend to be richer in sulphide than the peridotites.

The sample suite collected by the Creasy Group tends to have Cu contents in the range of the Fraser Zone main gabbros, with the exception of one gabbroic rock containing ~200 ppm Cu. Selected elements and element ratios from Nova drill core SFRD-0017 are plotted against depth in Fig. 14. The data illustrate that S and Cu contents vary based on rock type rather than stratigraphic level; i.e., S contents >10,000 ppm and Cu contents >500 ppm are confined to the gabbro-norites, irrespective of stratigraphic position.

Almost all rocks of the Fraser Zone are highly depleted in PGE relative to Ni and Cu, as expressed by Cu/Pd values mostly greater than 100,000. The highest value measured is 20 ppb Pt + Pd, and the most sulphide rich sample (with 8% sulphide) has a mere 10 ppb Pt + Pd. For the Creasy Group samples, PGE data are not yet available.

6.6. Strontium, Nd and S isotope geochemistry

In situ S isotope analysis of sulphides from 4 samples of Fraser Zone main gabbro yielded $\delta^{34}\text{S}$ values around 0 (Fig. 15), overlapping with the range of the mantle (–2 to +2, Ripley, 1999). In contrast, sulphides in samples from Nova have $\delta^{34}\text{S}$ values of 0 to +4 (Fig. 15). The whole-rock sulphur isotopic composition of sulphide-rich metasedimentary rocks of the Snowys Dam Formation (Arid Basin), sampled by drill core from the Sunline Prospect approximately 130 km northeast of Nova are $\delta^{34}\text{S}$ +3.6 to +5.2, overlapping with those from Nova itself.

In situ Sr isotope data are available for samples from the Nova SFRD0017 drill core and main gabbro from Mount Malcolm. All have enriched Sr isotopic signatures, with ϵ_{Sr} 38–52 at Nova and 17–32 at Mount Malcolm.

Only relatively limited variation is seen between the mafic-ultramafic rocks in the Fraser Zone in terms of Nd-isotopic compositions (Fig. 16). Five samples of main gabbro show a range in ϵ_{Nd} from 0.04 to –3.65. This range encompasses the range for the Group 1 hybrids (ϵ_{Nd} = –0.90 to –2.09; three samples), Group 2 hybrids (single sample with ϵ_{Nd} of –2.95) and samples from the Nova SFRD0017 drill core (ϵ_{Nd} = 0.43 to –1.29; three samples). When plotted against an incompatible trace-element ratio typically enriched in crustal material (e.g., La/Sm), the Nd-isotope data for all samples form an array consistent with mixing with available crustal components such as the Gora Hill Suite or felsic rocks formed during the Biranup Orogeny (Fig. 16).

Table 1

Average composition of Fraser Zone rocktypes.

	Fraser Zone main gabbros (liquids)	Fraser Zone Gp 2 hybrid (liquids)	Fraser Zone Gp 1 hybrid (liquids)	Nova peridotites (cumulates)	Nova gabbroonorites (cumulates)	Fraser Zone – Creasy peridotites
SiO ₂	48.91	54.09	48.77	42.18	49.26	41.04
TiO ₂	1.24	1.45	1.14	0.14	0.31	0.09
Al ₂ O ₃	16.45	15.76	16.13	6.39	15.37	6.11
Fe ₂ O ₃ T	11.63	11.30	11.86	13.63	8.97	14.00
MgO	8.46	4.62	9.04	31.47	13.07	34.66
MnO	0.20	0.21	0.21	0.19	0.15	0.20
CaO	9.98	8.05	9.78	4.16	11.16	2.84
K ₂ O	0.63	1.30	0.61	0.16	0.15	0.03
Na ₂ O	2.30	2.96	2.26	0.53	1.48	0.33
P ₂ O ₅	0.20	0.27	0.18	0.02	0.01	0.02
LOI	0.85	1.24	0.93	3.32	0.69	10.61
As	3.49	2.53	3.62	0.70		
Ba	292	730	236	31	51	16
Ce	30.17	47.54	26.51	2.90	3.71	1.49
Cr	220	113	316	1917	873	3174
Cs	0.46	0.20	0.97	0.57	0.12	0.10
Cu	51	40	49	154	691	45
Dy	4.95	6.27	4.48	0.61	1.25	0.26
Er	2.83	3.53	2.64	0.40	0.79	0.18
Eu	1.42	2.11	1.26	0.20	0.43	0.08
Ga	17.85	20.48	16.70	6.07	12.09	5.25
Gd	4.95	6.49	4.43	0.60	1.15	0.28
Hf	2.95	5.64	2.35	0.32	0.45	0.10
Ho	1.05	1.30	0.97	0.11	0.27	0.01
La	13.22	22.36	11.69	1.74	2.00	1.02
Lu	0.39	0.52	0.36	0.01	0.09	0.00
Nb	5.02	9.88	4.18	0.25	0.09	0.34
Nd	17.90	26.42	15.50	1.73	2.77	1.16
Ni	165	53	185	916	820	1219
Pb	7.52	12.63	6.97	0.41	3.30	0.29
Pr	3.75	5.83	3.27	0.40	0.55	0.28
Rb	16.53	21.20	20.37	6.16	2.19	1.36
Sc	33.13	29.36	29.52	12.74	31.00	1.24
Sm	4.36	6.21	3.83	0.46	0.86	0.29
Sn	0.54	0.41	0.52	2.60	1.68	0.00
S	689	211	728	2434	7163	1405
Sr	209	223	188	70	188	56
Ta	0.26	0.56	0.23			0.02
Tb	0.80	1.02	0.71	0.04	0.18	0.00
Th	0.95	0.49	1.66	0.24	0.08	0.04
U	0.26	0.24	0.43	0.18	0.01	0.03
V	192	184	188	72	189	50
Y	29.17	36.69	27.43	3.52	7.06	1.62
Yb	2.57	3.29	2.43	0.37	0.73	0.14
Zn	88	99	89	56	49	77
Zr	119	236	96	7	9	4

7. Discussion

7.1. Petrogenesis of the main gabbros

In order to gain a better understanding of the Ni–Cu–(PGE) prospectivity of the Fraser Zone and the Albany–Fraser Orogeny, it is important to constrain the nature of the mantle source and the crystallisation history of the parent magmas to the rocks. The combined whole rock and mineral compositional data suggest that the Fraser Zone main gabbros crystallised from basaltic magma having approximately 8.8% MgO. Based on the trends in binary variation plots (Fig. 10), the gabbroic and ultramafic cumulates from the Nova SFRD0017 drill core crystallised from a magma of broadly similar composition. The intersection of the tie lines with the MgO axis in the Al₂O₃/MgO plot suggests that olivine has MgO 40–45% (Fo 80–85), consistent with the available SEM data (Fo 80–83). Mineral compositional data for the samples of the Creasy Group of Companies are not yet available, but the higher Cr/V and Ni contents in the ultramafic Creasy samples suggest that these rocks may have crystallised from slightly more primitive magmas. Simulations using the thermodynamic program PELE (Boudreau, 1999) suggest that precipitates from average main

gabbro (at QFM and 5 kbar) consist of olivine of composition Fo 84, followed by orthopyroxene with En 84, clinopyroxene with Di 84, and plagioclase with An 70, i.e. compositions that overlap with those of the Nova minerals. Notably, if one would increase the modelling pressure to 8 kbar, orthopyroxene would be the first liquidus phase (En 87) followed by clinopyroxene (Di 85) and plagioclase (An 66), inconsistent with the observed crystallisation sequence and mineral compositions. This suggests that the main gabbro was emplaced at depths shallower than 20 km, or that it recrystallised during exhumation.

The least evolved main gabbros (Mg# 72–77, GSWA 183652 and 183669) have Th, U, and REE concentrations greater than N-MORB, but are strongly depleted in Nb and Ta (Fig. 11). This suggests that the parental magmas to the Fraser Zone gabbros were likely derived from a mantle source that was more depleted than the source to N-MORB. Jolly et al. (2001) used concentrations of Nb and Yb in basalt, normalised to 9 wt% MgO, to estimate the degree of mantle partial melting. A similar treatment of the data for the main gabbros suggests that the parent melts could have formed through <10% partial melting of a garnet-free spinel lherzolite mantle. This figure is possibly slightly low considering the rather high MgO content (>13 wt%) and moderate Mg# (up to

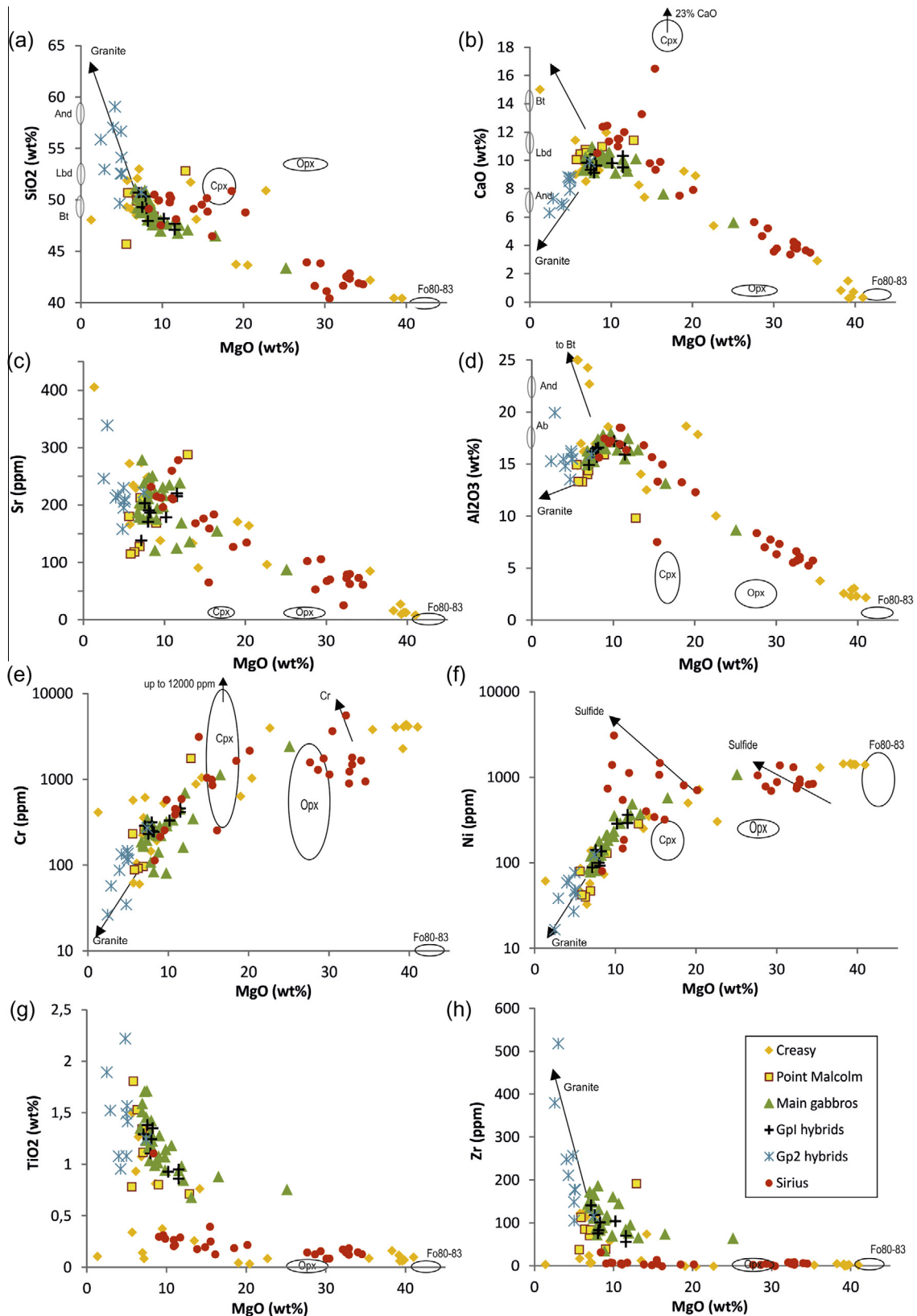


Fig. 10. (a–h) Binary whole rock variation diagrams vs MgO of (a) SiO₂, (b) CaO, (c) Sr, (d) Al₂O₃, (e) Cr, (f) Ni, (g) TiO₂, and (h) Zr. Composition of main minerals are indicated. Arrows denote compositional trend interpreted to result from contamination, sulphide or chromite accumulation. Bt = bytownite, Lbd = labradorite, Ab = albite, And = andesine.

71) in some of the non-cumulate rocks. However, the relatively low concentrations of Cr in the least evolved non-cumulate gabbros (<700 ppm) suggest that some clinopyroxene remained in the

mantle source after melting. This would limit the degree of melting to well below 20% (e.g., Sinton et al., 2003). Such relatively low degrees of partial melting of a depleted mantle could potentially

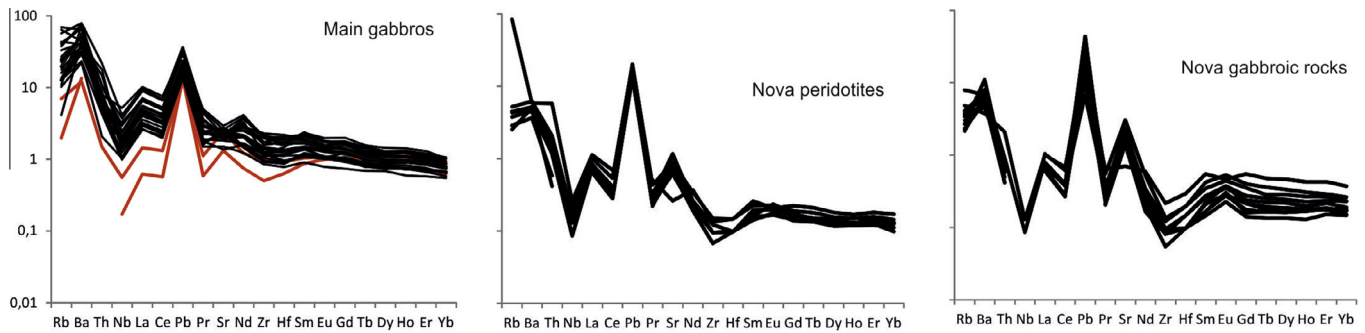


Fig. 11. N-MORB normalised multi-element plots of Fraser Zone main gabbros and peridotites and gabbroic rocks from Nova (normalisation factors from Sun and McDonough (1989)).

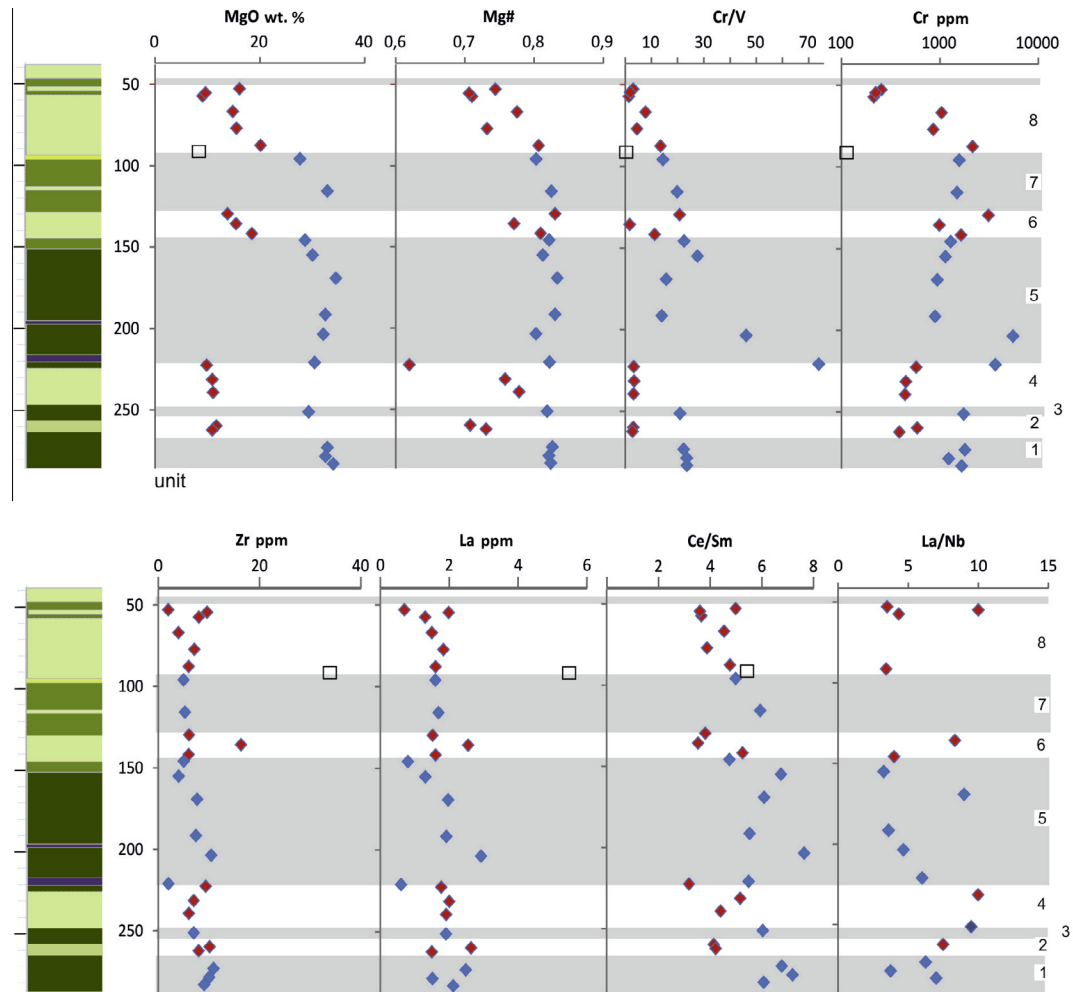


Fig. 12. Variation of selected major and trace element concentrations and ratios in drill core SFRD0017. Square symbol = dolerite.

explain the ultralow PGE contents in the Fraser Zone magmas and cumulates as the complete dissolution of mantle sulphide is thought to require more than approximately 20% partial melting (Barnes et al., 2015; Keays, 1995; Mungall and Brenan, 2014). Hamlyn et al. (1985) have argued that boninites and other magmas derived from depleted mantle have relatively high PGE contents, but more recent high precision data on boninites show them to be relatively PGE poor (Woodland et al., 2002).

The enrichments in Th and LREE relative to HFSE and HREE in the primitive gabbros are characteristic of subduction-related magmas. Such patterns formed the basis of the model of Condie and Myers (1999) who interpreted the gabbros of the Fraser Zone

to have formed in an oceanic arc setting. However, an oceanic setting can be discounted since geochronological, isotopic and geochemical data show that the same felsic crustal material lies on both sides of the Fraser Zone and includes Archean crust and granites derived through recycling of Archean crust prior to and during the Biranup Orogeny (Kirkland et al., 2011a; Spaggiari et al., 2015; Smithies et al., 2015). In addition, the Fraser gabbros themselves intrude a clastic sedimentary sequence (Snowys Dam Formation) interpreted as initially deposited within a foreland basin no more than 20 million years prior to intrusion (Spaggiari et al., 2015). Subduction-like trace element patterns can result through assimilation of crust by mantle-derived magmas. This model

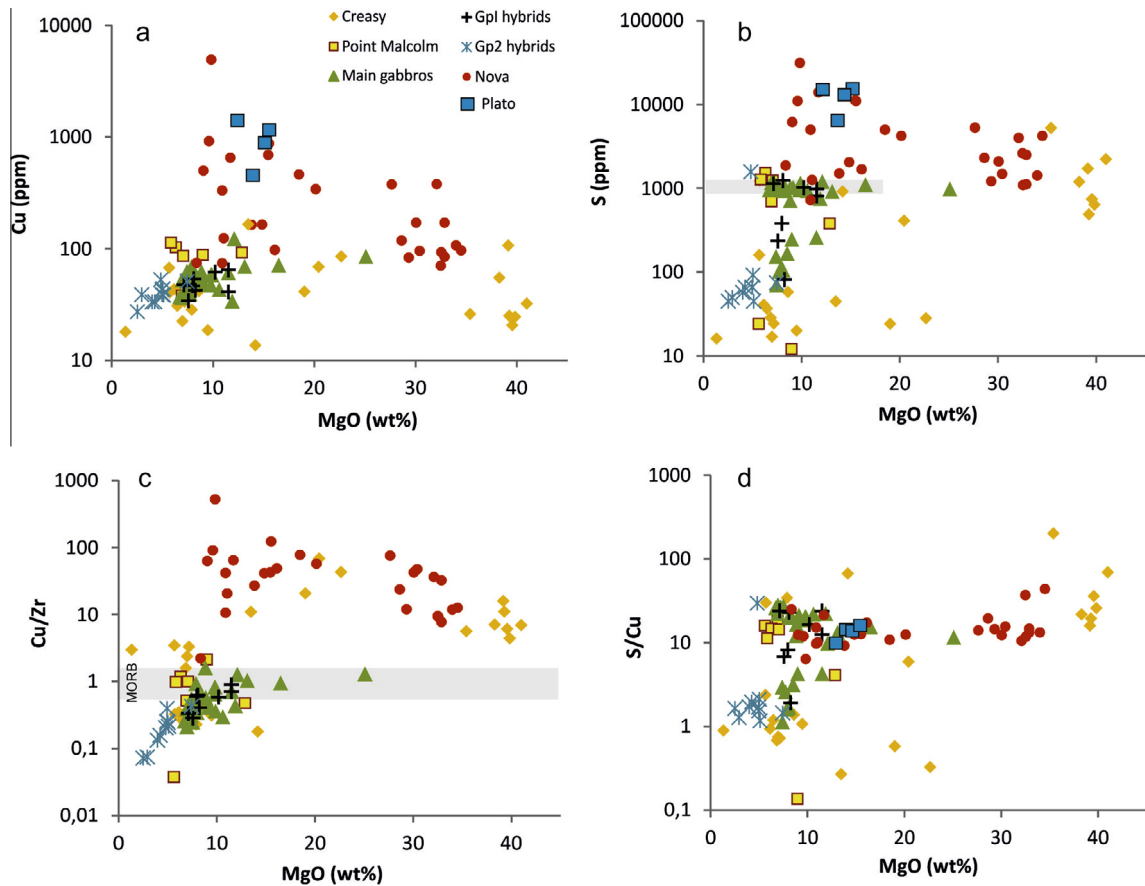


Fig. 13. Binary whole rock variation diagrams of chalcophile elements plotted vs MgO for Fraser Zone mafic and ultramafic rocks. Also included are data from the Plato prospect (Enterprise Metals, 2014).

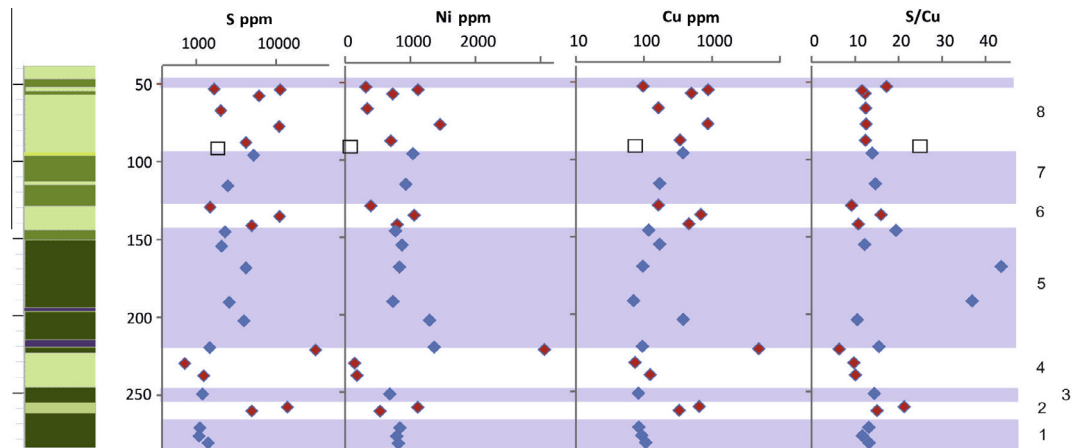


Fig. 14. Compositional variation vs height of S and selected chalcophile elements and element ratios in drill core SFRD0017. Square symbol = dolerite.

would be more consistent with the geological and geochemical data presented here. Earlier modelling has shown that the average trace element characteristics of main gabbro can be reproduced if a magma derived from a depleted mantle source is contaminated by <10% locally available Biranup basement (Smithies et al., 2013).

The least evolved main gabbros have La/Nb \sim 2.7 (Fig. 17), which are higher than primitive mantle values of \sim 1.0 (Sun and McDonough, 1989). This is indicative of crustal contamination. However, these ratios decrease slightly with decreasing Mg#, indicating that further compositional evolution does not involve further addition of crustal material.

7.2. Petrogenesis of the hybrid gabbros

The hybrid gabbros can be sub-divided into two groups that form distinct high- and low-La/Th trends broadly enveloping the field for the main gabbros (Fig. 17). This suggests that the hybrid gabbros formed through two distinct and unrelated processes. It is also apparent, both from field observation and from the typically higher Mg# in the main gabbros, that the latter do not simply represent mixtures between the two groups of hybrid gabbro. Importantly, examples of each hybrid group occur at many sampling sites and thus the petrogenetic processes involved are not isolated phenomena.

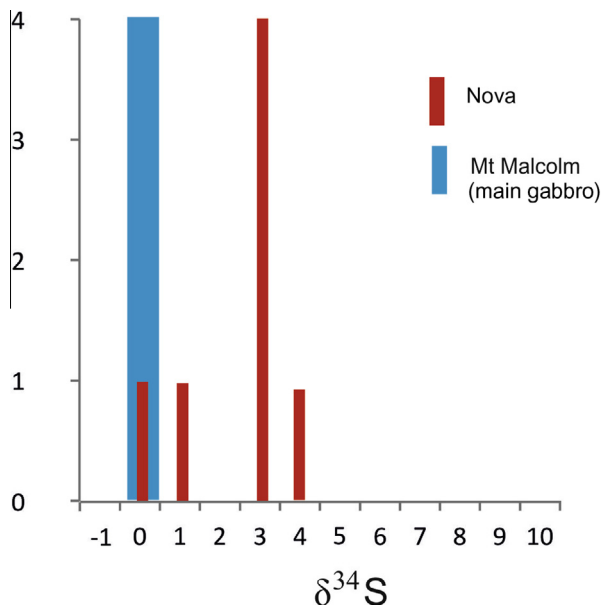


Fig. 15. Histogram of S isotope data from Mt Malcolm and Nova.

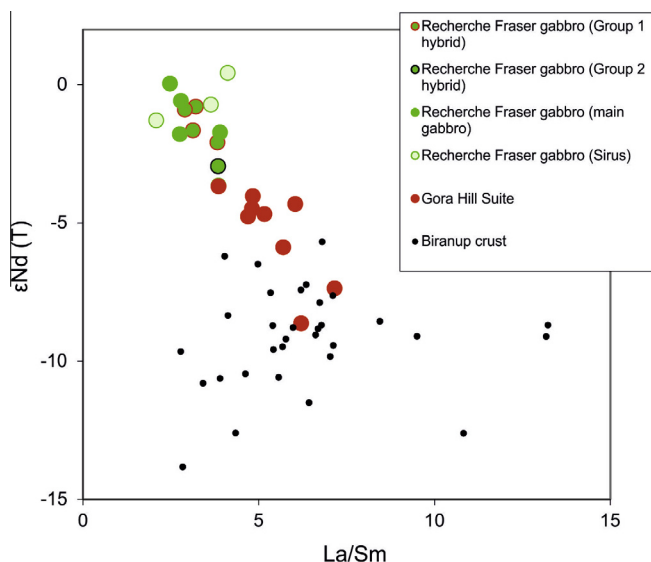


Fig. 16. Nd isotopes of Fraser Zone rocks plotted vs La/Sm.

Field observations indicate that the Group 2 hybrid gabbros have physically incorporated (e.g., mingled with) felsic material at the level of intrusion, but such evidence is not found in the case of Group 1 hybrids. Group 2 hybrids are typically significantly enriched in SiO₂ and have much lower Mg#, consistent with the field evidence for mingling. Group 1 hybrids cover the same range of SiO₂ concentrations and Mg# values as the main gabbros, although they range to higher concentrations of incompatible trace elements. A range of incompatible trace element variation diagrams (in particular, Th vs K or LREE, Fig. 18a) show that the Group 1 hybrids consistently plot to the more ‘crustal’ side (i.e., high Th) of the main gabbros and the simplest explanation for these hybrids is that they define the upper limit of early contamination by partial melts of Biranup crust seen in the main gabbros.

In contrast, Group 2 hybrids are defined by distinctly lower Th/K, Th/Pb, and Th/LREE ratios than both Group 1 hybrids and the main gabbros (Fig. 18a). On incompatible trace element variation diagrams only the most primitive granodioritic end members of the Gora Hill Suite consistently lie on the Group 2 hybrid trend.

This granodioritic component of the Gora Hill Suite is itself restricted to the Fraser Zone. Thus, it seems likely that Group 2 hybrids are local physical mixes of co-magmatic main gabbro and Gora Hill granodiorite. Such a process also explains the low S and Cu, and high Zr concentrations in the Group 2 hybrids – these being characteristics of the Gora Hills granodiorite. Such interaction is clearly rare and produces only minor magma volumes (see Fig. 19).

7.3. Constraints on the petrogenesis of the Nova deposit

The composition of the Nova sulphides and silicates can be reasonably related to the Fraser main gabbros assuming fractional crystallization and sulphide segregation at an average *R* factor (mass ratio of sulphide melt to silicate melt, Campbell and Naldrett, 1979) of ~1500, assuming a *D*_{sulphide melt/silicate melt} of 1000 for Cu, 500 for Ni and 30,000 for Pt. The modelled metal tenors are ~3.4% Cu, 4.5% Ni, 270 ppb Pt and 150 ppb Pd (Electronic Appendix 3). These tenors are broadly overlapping with the published data from the deposit (Bennett et al., 2014), except that our sulfides have slightly higher Cu/Ni. Possibly, the sulfides in the intrusion underwent some degree of fractionation, with the disseminated sulphides in the upper portion of the intrusion being relatively enriched in ISS component. Notably, PGE tenors in the Nova sulfides are amongst the lowest in magmatic sulphides globally.

The rocks from Nova differ from most other mafic–ultramafic rocks of the Fraser Zone, including the main gabbros, in several ways. Firstly, based on their low Zr, Ti and K contents, yet high Cr contents, the Nova samples are interpreted as cumulates, irrespective of rock type, whereas the regional gabbros are almost exclusively non-cumulates, showing relatively high concentrations of incompatible elements (Fig. 10). Secondly, the high Cu/Zr and S contents in all Nova rocks (Fig. 13) indicate that they contain cumulus magmatic sulphides (up to 8%), notwithstanding differentiation state, suggesting that the rocks crystallised from a magma saturated in sulphide melt. In contrast, the regional gabbroic rocks are exceedingly sulphide poor, consistent with Cu/Zr around or below unity, and likely crystallised from magma undersaturated in sulphide melt. Thirdly, the Nova rocks have a more pronounced crustal signature than the regional gabbroic rocks, expressed by their more radiogenic initial Sr isotopic compositions and relatively heavy S isotope signatures (Fig. 15). Preliminary indications are that this is likely due to additional late contamination with sedimentary rocks in which Sr and S isotopes underwent pronounced fractionation. The crustal source of sulphur had a similar composition as sedimentary rocks of the Snowys Dam Formation, suggesting assimilation of sulphidic sedimentary rocks that occur interlayered with the mafic–ultramafic rocks and occur both regionally and in the vicinity of the deposit.

Notably, the available Nd-isotopic data suggest that all mafic and ultramafic rocks sampled from the Fraser Zone (i.e., main and hybrid gabbros, as well as Nova mafic and ultramafic cumulates) could be derived from a similar bulk source composition. Confirming this using incompatible trace element geochemistry is problematic because the cumulate nature of the peridotites from the Nova SFRD0017 drill core means that many of the most strongly incompatible trace elements (and particularly Th and Nb) are at concentration levels close to analytical detection levels. However, plots of Pb/K₂O, Pb/Zr, Pb/LREE, Zr/Hf, LREE/Zr and P₂O₅/Pb employ pairs of trace elements that are of similar incompatibility within mafic and ultramafic magmas, have concentrations significantly higher than the analytical levels of detection, and that reflect magmatic (rather than cumulate) compositions. On compositional variation diagrams employing these ratios, cumulate samples from the Nova SFRD0017 drill core and several (but not all) Creasy Group peridotites form trends that

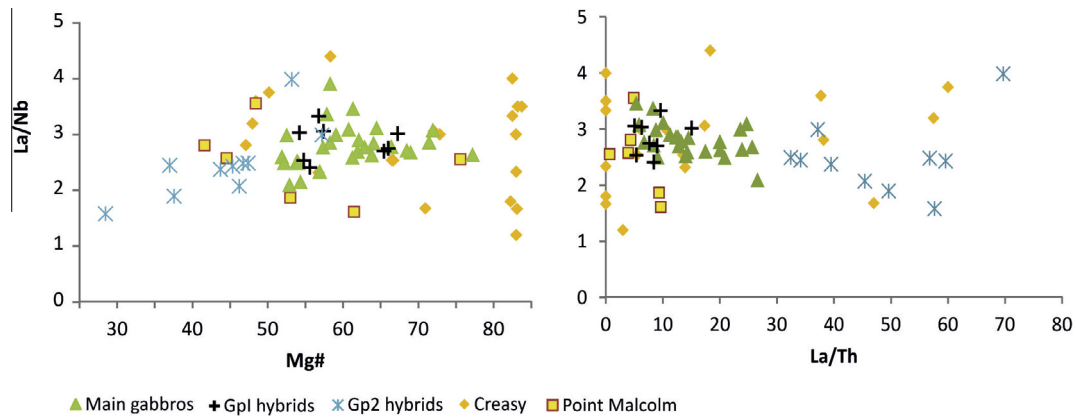


Fig. 17. Ratio diagrams of (a) La/Nb vs Mg# (b) La/Nb vs La/Th for mafic-ultramafic rocks from the Fraser Zone. Note that all Fraser Zone gabbros have elevated La/Nb relative to primitive mantle, likely indicative of crustal contamination, but La/Nb remains constant with falling Mg#, interpreted to reflect lack of *in situ* contamination. Also note difference in composition between Gpl and GpII hybrids.

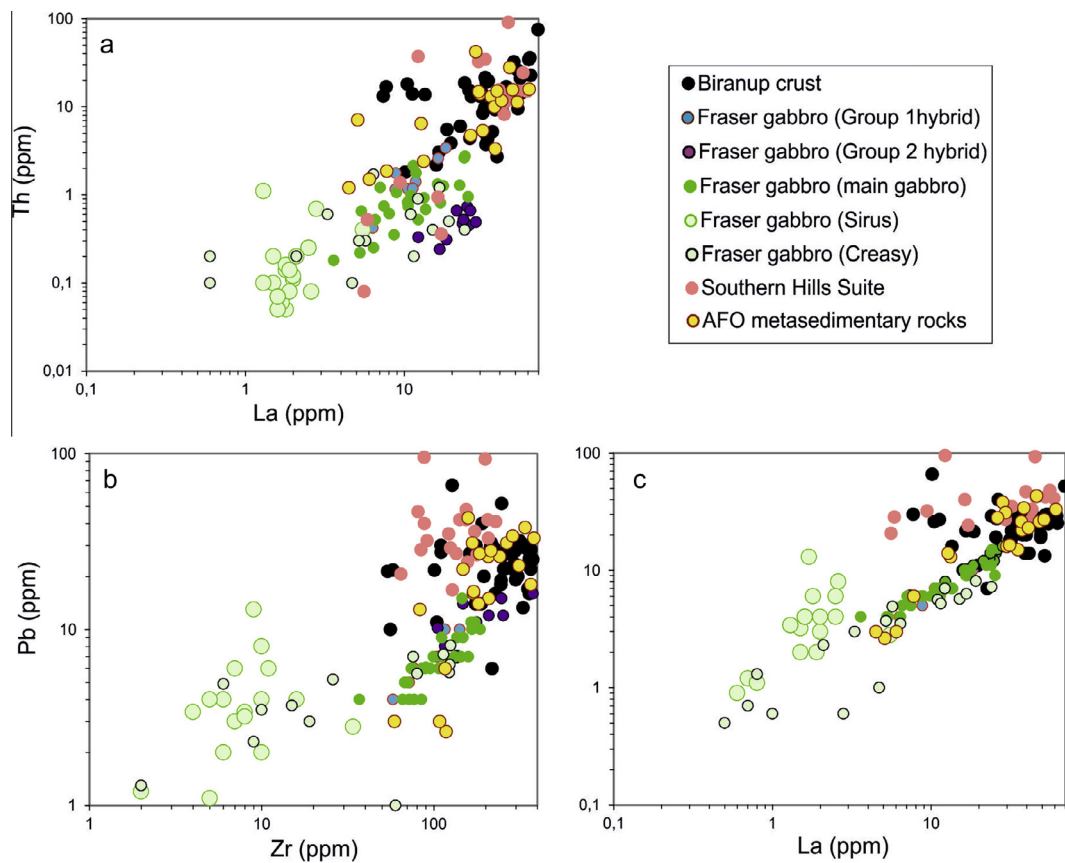


Fig. 18. Binary variation diagrams of (a) Th vs La, (b) Pb vs Zr, and (c) Pb vs La. Note contrasting compositional fields of main and hybrid gabbros in (a). In (b) and (c) samples from Nova and ultramafic rocks from the Creasy Group of companies define trends that are distinct from those of the main and hybrid gabbros. This is best explained by contamination with either granites of the Southern Hills Suite or the Arid Basin sedimentary rocks.

are distinct from those of the main gabbros and hybrid gabbros (Fig. 18b and c). These differences cannot simply reflect differing degrees of fractional crystallisation within a common parental liquid because the concentrations of some trace elements (e.g., Pb) show significant overlap between the two populations and because for plots of, e.g., LREE/Zr and LREE/K₂O, joining the two trends would produce curved trends that contradict the relative incompatibility of the element pairs within mafic and ultramafic magmas. These differences in trace element ratios require either a different source or a different (or additional) contaminant. In all cases when the Nova trace element trends are compared with

geochemical data from the available range of felsic crustal lithologies, contamination of the Nova magmas with Arid Basin sedimentary rocks or with granites of the Southern Hill Suite (i.e., melts of the Arid Basin sedimentary rocks) provide the most viable interpretations (Fig. 18b and c). This is an important conclusion because the S-isotopic data also suggest that the Nova SFRD0017 rocks derived sulphur from the same crustal source.

The interlayering of mafic and ultramafic rocks at Nova could suggest that both lithologies are cumulates formed within a cyclically layered intrusion, as a result of alternating fractionation and recharge. However, this model is inconsistent with the fact that

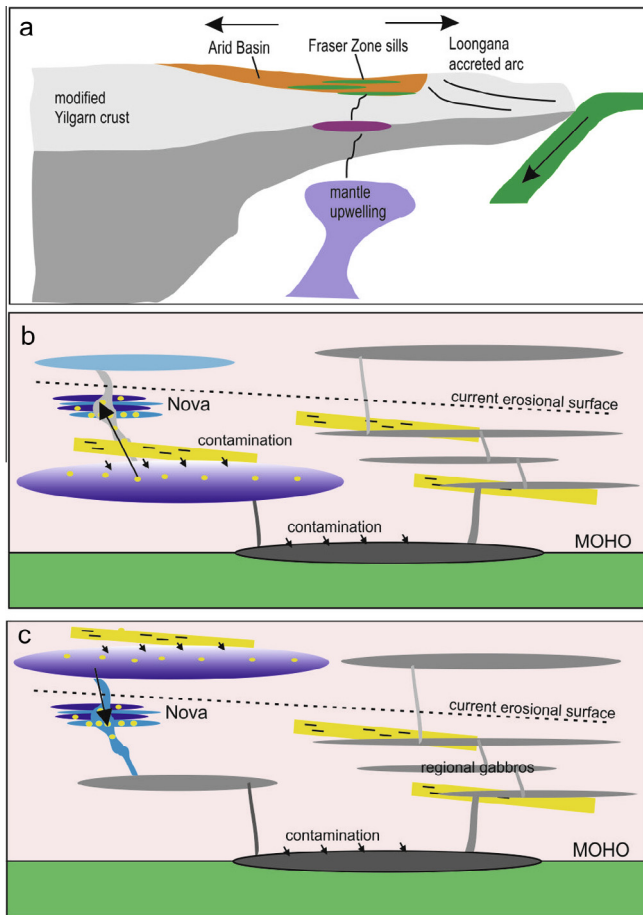


Fig. 19. Metallogenic model, based on currently available information. (a) Regional setting of Fraser Zone magmatism at the southeastern margin of the Yilgarn craton, formed in response to west-directed thrusting and accretion of the Loongana oceanic arc of the Madura Province onto the passive margin of the Albany–Fraser Orogen (Spaggiari et al., 2015). Continued convergence may have initiated west-dipping subduction beneath the passive margin and accreted arc, and the formation of a distal back-arc regime in the current position of the Fraser Zone (Spaggiari et al., 2015). (b) Sketch showing preferred model for formation of Nova deposit via ascent of sulfidic crystal slurries derived from a large staging chamber where abundant crustal melting and sulfide assimilation occurred. Magma ascent was triggered by tectonism. Regional mafic–ultramafic sills are unmineralised despite having intruded granitic basement and sulfidic sedimentary rocks, because they are not fed from staging chambers that underwent sulfide assimilation. (c) Alternative model of formation of Nova deposit, via downward percolation of sulfidic slurries from an eroded staging chamber.

the gabbro-norites have broadly similar Cu/S as the ultramafic cumulates and higher sulphide contents. Fractionation of a magma saturated in sulphide melt would be expected to result in progressive metal depletion of the magma (i.e., decreasing Cu/S) and lower sulphide contents in gabbro-norites than ultramafic rocks as the slope of the S saturation curve is relatively shallow once plagioclase has appeared on the liquidus (Ripley and Li, 2013). Thus, the S and Cu contents of the rocks could be more readily explained if the gabbros and peridotites were emplaced as distinct sills of crystal- and sulphide-charged slurries (Fig. 19). Other proposed examples for emplacement of sulfide-bearing ultramafic slurries include Kabanga and the recently discovered Xiarihamu Ni–Cu deposit, China (Li et al., 2015). The lack of chilled margins at the contacts between the mafic and ultramafic rocks could be explained by overlap in emplacement age and because intrusion happened at near granulite facies conditions. This model is consistent with the occurrence of variably sulphide mineralised pyroxenite fragments within coarse gabbroic rocks (sample GSWA 201255).

Such textures suggest a relatively dynamic emplacement environment in which the ascending magma can entrain fragments of earlier intrusive phases forming the wall rocks to the conduits.

The sequence of intrusion of the sills remains unclear. The relatively fine grain size of some of the gabbroic rocks could suggest that the gabbros intruded first, followed by pulses of olivine rich magmas that injected into the still hot gabbroic complex. This sequence of intrusion would be consistent with the presence of coarse grained gabbros containing inclusions of finer grained norite and pyroxenite, and it is analogous to the sequence of emplacement at, e.g., the Kabanga Ni sulphide deposit in Tanzania (Maier and Barnes, 2010) or the Bushveld Complex (Eales and Cawthorn, 1996).

But why are most of the other sills in the region non-cumulates and barren of sulphide, even though sulphidic sedimentary rocks of the Arid Basin are relatively common? Two possibilities may be considered. First, the relatively thin main gabbro sills may have cooled too fast to undergo significant fractionation and to trigger significant melting of the sedimentary host rocks, whereas the relatively thick Nova sill complex cooled slower allowing more assimilation of the host rocks. If the emplacement depth was in a granulite facies regime at 25–30 km depth, the heat flux from the intrusions into the country rocks should have been relatively low, but it remains a strong possibility that the measured P–T conditions on the metasedimentary rocks are the result of post magmatic metamorphism and that the emplacement depth of the Nova sills was significantly shallower, as indicated earlier. Alternatively, or additionally, assimilation could have been controlled by mechanical rather than chemical and thermal erosion, favouring the dynamically emplaced crystal-charged Nova magmas.

7.4. Ni–Cu sulphide prospectivity of the Albany–Fraser Orogen

The Albany–Fraser Orogen offers an opportunity to examine the complexity of craton margin environments and the related potential for magmatic mineralisation. Begg et al. (2010) suggested that craton margins are particularly prospective for magmatic Ni–Cu (PGE) deposits because mantle plumes are diverted to these regions by the thick cratonic keels, and because craton margins feature abundant large fractures and weak zones through which magmas can ascend. The Fraser Zone lies within the reworked margin of the Yilgarn Craton and possibly developed in response to accretionary and extensional processes occurring along that margin at c. 1330–1300 Ma, shortly thereafter followed by a period of compression (e.g., Clark et al., 2014; Spaggiari et al., 2014a, 2015). Given the dynamic plate tectonic environment and the widespread occurrence of magmatism exhibited by the 1330–1280 Ma Recherche Supersuite a mantle plume is probably the least likely explanation for Fraser Zone magmatism. However, the very large volume of mafic–ultramafic magma generated at c. 1300 Ma is of key importance in prospectivity. High grade metamorphic conditions contemporaneous with and resulting from mafic magmatism, and the interaction between mafic magmas and felsic magmas derived from melting of slightly older metasedimentary country rocks indicates an extremely hot and dynamic environment where assimilation of any sulphidic crust is favoured.

The highly depleted PGE contents (expressed by Cu/Pd mostly above 100,000) and the relatively low Cu in all Fraser Zone rocks (30% lower than average MORB) can potentially be explained by relatively small degree mantle melting (<20%) during which sulphides are incompletely dissolved in the magma, analogous to many other samples of MORB (e.g., Yang et al., 2014). Importantly, this has no impact on the Ni prospectivity of the magmas, as Ni in the mantle is largely controlled by olivine rather than sulphide. An alternative explanation for the low PGE content of the magmas

could be that fertile basaltic magmas equilibrated with small amounts of sulphide prior to emplacement, e.g., in response to contamination in the lower crust during which the highly chalcophile Cu and PGE were extracted relatively efficiently in segregating sulphide melts compared to Ni ($D_{\text{sulphide melt-basalt}}$ is $>10^4$ for PGE, ~ 1000 for Cu, vs 300–500 for Ni, Barnes and Lightfoot, 2005). This idea would be consistent with the model of Chiaradia (2014) who explained low Cu contents in some arc basalts via sulphide fractionation during ascent through thick crust. However, we argue that this model is incompatible with the remarkable regional homogeneity of the Fraser Zone magmas in terms of their chalcophile element depletion; Crustal interaction rarely results in homogenous metal depletion in magma suites as some magma pulses that use conduits lined by earlier magmatic phases can be effectively shielded from contamination.

The compositional similarity between the Nova samples, many of the Creasy Group samples, and the limited data available from the Plato prospect of Apollo Minerals, in terms of their elevated sulphide content, their cumulate nature, and their high Cr/V and Ni content, could suggest that the entire Fraser Zone is relatively prospective for Ni–Cu sulphides. The lower sulphide contents in the Creasy Group samples may reflect less contamination with sulphur-bearing metasedimentary country rock, but verification of this model requires S and Sr isotope data.

8. Summary and conclusions

Exploration of the extensive Albany–Fraser Orogen at the south eastern margin of the Yilgarn Craton is in its infancy. The present study indicates that the Fraser Zone magmatism formed by moderate degrees ($<20\%$) of melting of a source more depleted than N-MORB. Mantle melting was driven by plate motions. The relatively low degree of mantle melting led to incomplete dissolution of mantle sulphides and ultra-low PGE contents of the magmas and cumulates. The magmas were ponded and crustally contaminated in the lower to mid crust where they formed abundant sills (Fig. 19). An intrusion belonging to this suite hosts the recently discovered Nova Ni deposit, suggesting that the Fraser Zone has the potential to become a significant new Ni camp. Critical factors in sulphide prospectivity include the craton margin setting within an orogenic belt, the presence of large volumes of mafic–ultramafic magmas resulting in a high heat flux to the crust, and the presence of sulphide bearing sedimentary rocks that can provide external S to the magmas. We suggest as one possible working hypothesis that the sulphide melt initially formed in large magma chambers due to roof assimilation. Periodic ejections of crystal and sulphide charged magmas from these staging chambers, possibly driven by seismic pumping triggered by tectonism, formed mineralised sills at higher crustal levels such as Nova (Fig. 19). Barren sills are not derived from large staging chambers and thus formed from relatively crystal-poor magma that cooled relatively fast and thus tend to be relatively fine grained and sulphide poor. An alternative hypothesis could be that the Nova sulphides percolated downward from a now eroded magma chamber. Further evaluation of these hypotheses awaits access to, and detailed study of the ore deposit itself.

Acknowledgements

We are indebted to the Creasy Group of Companies for discussions and the donation of data and samples generated through industry exploration of the greater Fraser Range. HS and CS publish with the permission of the Executive Director of the Geological Survey of Western Australia. We thank Marco Fiorentini and an anonymous reviewer for their constructive comments.

Appendix A. Supplementary data

Supplementary data associated with this article can be found, in the online version, at <http://dx.doi.org/10.1016/j.precamres.2016.05.004>.

References

- Barnes, S.-J., Lightfoot, P.C., 2005. Formation of magmatic nickel sulfide deposits and processes affecting their copper and platinum group element contents. *Econ. Geol.* 100, 179–214.
- Barnes, S.-J., Maier, W.D., Curl, E., 2010. Composition of the marginal rocks and sills of the Rustenburg layered suite, Bushveld Complex, South Africa: implications for the formation of the PGE deposits. *Econ. Geol.* 105, 1491–1511.
- Barnes, S.J., Cruden, A.R., Saumur, B.-M., Arndt, N.T., 2015. The mineral system approach applied to magmatic Ni–Cu–PGE sulphide systems. *Ore Geol. Rev.* <http://dx.doi.org/10.1016/j.oregeorev.2015.06.012>.
- Begg, G.C., Hronsky, J.A.M., Arndt, N.T., Griffin, W.L., O'Reilly, S.Y., Hayward, N., 2010. Lithospheric, cratonic and geodynamic setting of Ni–Cu–PGE sulfide deposits. *Econ. Geol.* 105, 1057–1070.
- Bennett, M., Gollan, M., Staubmann, M., Bartlett, J., 2014. Motive, means, and opportunity: key factors in the discovery of the Nova-Bollinger magmatic nickel-copper sulfide deposits in Western Australia. *Soc. Econ. Geol. Spec. Publ.* 18, 301–320.
- Boudreau, A.E., 1999. PELE—a version of the MELTS software program for the PC platform. *Comput. Geosci.* 25, 201–203.
- Campbell, I.H., Naldrett, A.J., 1979. The influence of silicate:sulfide ratios on the geochemistry of magmatic sulfides. *Econ. Geol.* 74, 1503–1505.
- Cassidy, K.F., Champion, D.C., Krapez, B., Barley, M.E., Brown, S.J.A., Blewett, R.S., Groenewald, P.B., Tyler, I.M., 2006. A Revised Geological Framework for the Yilgarn Craton, Western Australia. Western Australia Geological Survey, Record 2006/8, p. 8.
- Chiaradia, M., 2014. Copper enrichment in arc magmas controlled by overriding plate thickness. *Nat. Geosci.* 7, 43–46.
- Clark, D.J., Hensen, B.J., Kinny, P.D., 2000. Geochronological constraints for a two-stage history of the Albany–Fraser Orogen, Western Australia. *Precamb. Res.* 102, 155–183.
- Clark, C., Kirkland, C.L., Spaggiari, C.V., Oorschot, C., Wingate, M.T.D., Taylor, R.J., 2014. Proterozoic granulite formation driven by mafic magmatism: an example from the Fraser Range Metamorphics. *Western Aust.* 240, 1–21.
- Condie, K.C., Myers, J.S., 1999. Mesoproterozoic Fraser Complex: geochemical evidence for multiple subduction-related sources of lower crustal rocks in the Albany–Fraser Orogen, Western Australia. *Aust. J. Earth Sci.* 46, 875–882.
- Eales, H.V., Cawthorn, R.G., 1996. The Bushveld complex. In: Cawthorn, R.G. (Ed.), *Layered Intrusions*. Elsevier, Amsterdam, pp. 181–229.
- Enterprise Metals, 2014. Fraser Range Project, Exploration Licence 63/1281, Final Drilling Report, Co-funded Drilling Agreement DAG 2014/00384566, 25th July 2014. Department of Mines and Petroleum, Perth.
- Fornoni Candia, M.A., Mazzucchelli, M., Siena, F., 1989. Sub-solidus reactions and corona structures in the Niquelândia layered complex (Central Goiás, Brazil). *Mineral. Petrol.* 40, 17–37.
- Gale, A., Dalton, C.A., Langmuir, C.H., Su, Y., Schilling, J.-G., 2013. The mean composition of ocean ridge basalts. *Geochem. Geophys. Geosyst.* 14, 489–518.
- Gilbert, S.E., Danyushevsky, L.V., Rodermann, T., Shimizu, A., Gurenko, A., Meffre, S., Thomas, H., Large, R.R., Death, D., 2014. Optimisation of laser parameters for the analysis of sulphur isotopes in sulphide minerals by laser ablation ICP-MS. *J. Anal. At. Spectrom.* 29, 1042–1051.
- Glikson, A.Y., Stewart, A.T., Ballhaus, G.L., Clarke, G.L., Feeken, E.H.T., Level, J.H., Sheraton, J.W., Sun, S.-S., 1996. Geology of the western Musgrave Block, central Australia, with reference to the mafic–ultramafic Giles Complex. *Aust. Geol. Surv. Org. Bull.* 239, 206p.
- Gollan, M., 2012. Final Drilling Report 'The Eye'. Sirius Gold Pty Ltd, Geological Survey of Western Australia, Statutory Mineral Exploration Report, A092733 (unpublished).
- Hamlyn, P.R., Keays, R.R., Cameron, W.E., Crawford, A.J., Waldron, H.M., 1985. Precious metals in magnesian low-Ti lavas: implications for metallogenesis and sulfur saturation in primary magmas. *Geochim. Cosmochim. Acta*.
- Jolly, W.T., Lidiak, E.G., Dickin, A.P., Wu, T.-U., 2001. Secular geochemistry of central Puerto Rican island arc lavas: constraints on Mesozoic tectonism in the eastern Greater Antilles. *J. Petrol.* 42, 2197–2214.
- Keays, R.R., 1995. The role of komatiitic and picritic magmatism and S-saturation in the formation of ore deposits. *Lithos* 34, 1–18.
- Kirkland, C.L., Spaggiari, C.V., Pawley, M.J., Wingate, M.T.D., Smithies, R.H., Howard, H.M., Tyler, I.M., Belousova, E.A., Poujol, M., 2011a. On the edge: U–Pb, Lu–Hf, and Sm–Nd data suggests reworking of the Yilgarn Craton margin during formation of the Albany–Fraser Orogen. *Precamb. Res.* 187, 223–247. <http://dx.doi.org/10.1016/j.precamres.2011.03.002>.
- Kirkland, C.L., Spaggiari, C.V., Smithies, R.H., Wingate, M.T.D., 2014. Cryptic progeny of craton margins: geochronology and isotope geology of the Albany–Fraser Orogen with implications for evolution of the Tropicana zone. In: Albany–Fraser Orogen Seismic and Magnetotelluric (MT) Workshop 2014: Extended Abstracts: Compiled by Spaggiari CV and Tyler IM. Geological Survey of Western Australia, Record 2014/6, pp. 89–101.

- Li, C., Zhang, Z., Li, W., Wang, Y., Sund, T., Ripley, E.M., 2015. Geochronology, petrology and Hf–S isotope geochemistry of the newly-discovered Xiarihamu magmatic Ni–Cu sulfide deposit in the Qinghai–Tibet plateau, western China. *Lithos* 216–217, 224–240.
- Lightfoot, P.C., Naldrett, A.J., 1983. The geology of the Tabankulu section of the Insizwa Complex, Transkei, Southern Africa, with reference to the nickel sulphide potential. *Trans. Geol. Soc. S. Afr.* 86, 169–187.
- Maier, W.D., Barnes, S.-J., 2010. The Kabanga Ni sulfide deposits, Tanzania: II. Chalcophile and siderophile element geochemistry. *Miner. Deposita* 45, 443–460.
- Maier, W.D., Eales, H.V., 1997. Correlation within the UG2–Merensky Reef interval of the Western Bushveld Complex, based on geochemical, mineralogical and petrological data. *Geol. Surv. S. Afr. Bull.* 120, 56.
- Maier, W.D., Howard, H.M., Smithies, R.H., Yang, S.H., Barnes, S.-J., O'Brien, H., Huhma, H., Gardoll, S., 2015. Magmatic ore deposits in mafic–ultramafic intrusions of the Giles Event, Western Australia. *Ore Geol. Rev.* <http://dx.doi.org/10.1016/j.oregeorev.2015.06.010>.
- Mole, D.R., Fiorentini, M.L., Thebaud, N., McCuaig, T.C., Cassidy, K.F., Kirkland, C.L., Wingate, M.T.D., Romano, S.S., Doublier, M.P., Belousova, E.A., 2012. Spatio-temporal constraints on lithospheric development in the southwest-central Yilgarn Craton, Western Australia. *Aust. J. Earth Sci.* 59, 625–656.
- Müller, W., Shelley, M., Miller, P., Broude, S., 2009. Initial performance metrics of a new custom-designed ArF excimer LA-ICPMS system coupled to a two-volume laser-ablation cell. *J. Anal. At. Spectrom.* 24, 209–214.
- Mungall, J., Brennan, J., 2014. Partitioning of platinum-group elements and Au between sulfide liquid and basalt and the origins of mantle–crust fractionation of the chalcophile elements. *Geochim. Cosmochim. Acta* 125, 265–289.
- Occhipinti, S.A., Doyle, M., Spaggiari, C.V., Korsch, R., Cant, G., Martin, K., Kirkland, C. L., Savage, J., Less, T., Bergin, L., Foz, L., 2014. Interpretation of the deep seismic reflection line 12GA–T1: northeastern Albany–Fraser Orogen. In: Albany–Fraser Orogen Seismic and Magnetotelluric (MT) Workshop 2014: Extended Abstracts Compiled by Spaggiari CV and Tyler IM. Geological Survey of Western Australia, Record 2014/6, pp. 52–68.
- Oorschot, C.W., 2011. P–T–t evolution of the Fraser Zone, Albany–Fraser Orogen, Western Australia. Geological Survey of Western Australia, Record 2011/18, p. 101.
- Raedeke, L.D., 1982. Petrogenesis of the Stillwater Complex (Ph.D. thesis). The University of Washington, Seattle, p. 212 (unpublished).
- Ramos, F.C., Wolff, J.A., Tollstrup, D.L., 2004. Measuring $^{87}\text{Sr}/^{86}\text{Sr}$ variations in minerals and groundmass from basalts using LAMC-ICPMS. *Chem. Geol.* 211, 135–158.
- Ramos, F.C., Wolff, J.A., Tollstrup, D.L., 2005. Sr isotope disequilibrium in Columbia River flood basalts: evidence for rapid shallow-level open-system processes. *Geology* 33, 457–460.
- Rankenburg, K., Lassiter, J.C., Brey, G., 2004. Origin of megacrysts in volcanic rocks of the Cameroon volcanic chain – constraints on magma genesis and crustal contamination. *Contrib. Mineral. Petrol.* 147, 129–144.
- Ripley, E.M., 1999. Systematics of sulphur and oxygen isotopes in mafic igneous rocks and related Cu–Ni–PGE mineralization. In: Keays, R.R., Leshner, C.M., Lightfoot, P.C., Farrow, C.E.G. (Eds.), *Dynamic processes in magmatic ore deposits and their application to mineral exploration*: Geological Association of Canada, Short Course Notes, vol. 13. Springer, NY, pp. 133–158.
- Ripley, E.M., Li, C., 2013. Sulfide saturation in Mafic magmas: is external sulfur required for magmatic Ni–Cu (PGE) ore genesis? *Econ. Geol.* 108, 45–58.
- Sinton, J.M., Ford, L.L., Chappell, B., McCulloch, M.T., 2003. Magma genesis and mantle heterogeneity in the Manus back-arc basin, Papua New Guinea. *J. Petrol.* 44, 159–195.
- Smithies, R.H., Spaggiari, C.V., Kirkland, C.L., Howard, H.M., Maier, W.D., 2013. Petrogenesis of Gabbros of the Mesoproterozoic Fraser Zone: Constraints on the Tectonic Evolution of the Albany–Fraser Orogen. Geological Survey of Western Australia, Record 2013/5, p. 29.
- Smithies, R.H., Spaggiari, C.V., Kirkland, C.L., Maier, W.D., 2014. Geochemistry and petrogenesis of igneous rocks in the Albany–Fraser Orogen. In: Albany–Fraser Orogen Seismic and Magnetotelluric (MT) Workshop 2014: Extended Abstracts Compiled by Spaggiari CV and Tyler IM. Geological Survey of Western Australia, Record 2014/6, pp. 77–88.
- Smithies, R.H., Spaggiari, C.V., Kirkland, C.L., 2015. Building the Crust of the Albany–Fraser Orogen; Constraints from Granite Geochemistry. Geological Survey of Western Australia, Report 150, p. 49.
- Sobolev, S.V., Sobolev, A.V., Kuzmin, D.V., Krivolutskaia, N.A., Petrunin, A.G., Arndt, N.T., Radko, V.A., Vasiliev, Y.R., 2011. Linking mantle plumes, large igneous provinces and environmental catastrophes. *Nature* 477, 312–316.
- Spaggiari, C.V., Bodorkos, S., Barquero-Molina, M., Tyler, I.M., Wingate, M.T.D., 2009. Interpreted bedrock geology of the south Yilgarn and central Albany–Fraser Orogen, Western Australia. Geological Survey of Western Australia, Record 2009/10, p. 84.
- Spaggiari, C.V., Kirkland, C.L., Pawley, M.J., Smithies, R.H., Wingate, M.T.D., Doyle, M. G., Blenkinsop, T.G., Clark, C., Oorschot, C.W., Fox, L.J., Savage, J., 2011. The Geology of the East Albany–Fraser Orogen – A Field Guide. Geological Survey of Western Australia, Record 2011/23, p. 97.
- Spaggiari, C.V., Kirkland, C.L., Smithies, R.H., Wingate, M.T.D., 2012. What lies beneath – interpreting the Eucla basement. In: GSWA 2012 extended abstracts: promoting the prospectivity of Western Australia. Geological Survey of Western Australia, Record 2012/2, pp. 25–27.
- Spaggiari, C.V., Kirkland, C.L., Smithies, R.H., Wingate, M.T.D., 2014a. Tectonic Links between Proterozoic Sedimentary Cycles, Basin Formation and Magmatism in the Albany–Fraser Orogen, Western Australia. Geological Survey of Western Australia, Report 133, p. 63.
- Spaggiari, C.V., Occhipinti, S.A., Korsch, R.J., Doublier, M.P., Clark, D.J., Dentith, M.C., Gessner, K., Doyle, M.G., Tyler, I.M., Kennett, B.L.N., Costelloe, R.D., Fomin, T., Holzschuh, J., 2014b. Interpretation of Albany–Fraser seismic lines 12GA–AF1, 12GA–AF2 and 12GA–AF3: implications for crustal architecture. In: Albany–Fraser Orogen Seismic and Magnetotelluric (MT) Workshop 2014: Extended Abstracts Compiled by Spaggiari CV and Tyler IM. Geological Survey of Western Australia, Record 2014/6, pp. 28–51.
- Spaggiari, C.V., Kirkland, C.L., Smithies, R.H., Wingate, M.T.D., Belousova, E., 2015. Transformation of an Archean craton margin during Proterozoic basin formation and magmatism: the Albany–Fraser Orogen, Western Australia. *Precamb. Res.* 266, 440–466.
- Sun, S.-S., McDonough, W.F., 1989. Chemical and isotopic systematics of oceanic basalts: implications for mantle compositions and processes. In: Saunders, A.D., Norry, M.J. (Eds.), *Magmatism in the Ocean Basins*, 42. Geological Society, London, Special Publication, pp. 313–345.
- Teigler, B., Eales, H.V., 1996. The lower and critical zones of the western limb of the Bushveld Complex, as indicated by the Nooitgedacht boreholes. *Geol. Surv. S. Afr. Bull.* 111, 126.
- Tyler, I.M., Spaggiari, C.V., Occhipinti, S.A., Kirkland, C.L., Smithies, R.H., 2014. The Albany–Fraser deep reflection seismic and MT survey: Implications for mineral systems. In: Albany–Fraser Orogen Seismic and Magnetotelluric (MT) Workshop 2014: Extended Abstracts Compiled by Spaggiari CV and Tyler IM. Geological Survey of Western Australia, Record 2014/6, pp. 174–182.
- Wallace, P., Carmichael, I.S.E., 1992. Sulfur in basaltic magmas. *Geochim. Cosmochim. Acta* 56, 1863–1874.
- Woodland, S.J., Pearson, D.G., Thirwall, M.F., 2002. A platinum group element and Re–Os isotope investigation of siderophile element recycling in subduction zones: comparison of Grenada, lesser antilles arc, and the Izu–Bonin arc. *J. Petrol.* 43, 171–198.
- Yang, S., Maier, W.D., Lahaye, Y., O'Brien, H., 2013. Strontium isotope disequilibrium of plagioclase in the Upper Critical Zone of the Bushveld Complex: evidence for mixing of crystal slurries. *Contrib. Mineral. Petrol.* <http://dx.doi.org/10.1007/s00410-013-0903-4>.
- Yang, A.Y., Zhou, M.-F., Zhao, T.-P., Deng, X.-G., Qi, L., Xu, J.-F., 2014. Chalcophile elemental compositions of MORBs from the ultraslow-spreading Southwest Indian Ridge and controls of lithospheric structure on S-saturated differentiation. *Chem. Geol.* 382, 1–13.